ISSN 2350-3432 (Online) ISSN 2463-6029 (Print)

Catchment and lake water quality modelling to assess management options for Lake Rerewhakaaitu

July 2020

ERI Report: 150

Client report prepared for Bay of Plenty Regional Council

By Eunju Cho, David P. Hamilton, Paul White and Chris G. McBride

Environmental Research Institute, The University of Waikato
Private Bag 3105, Hamilton 3240, New Zealand

Cite report as:

Cho[1], E., Hamilton[2], D. P., White[3], P., McBride, C. G. (2019). Catchment and lake water quality modelling to assess management options for Lake Rerewhakaaitu. ERI Report 150. Environmental Research Institute, University of Waikato, Hamilton, New Zealand. 43 pp.

1. Current affiliation: n/a
2. Current affiliation: Australian Rivers Institute, Griffith University, Nathan Qld 4111, Australia
3. Geological & Nuclear Sciences Ltd, Taupo
4. Environmental Research Institute, The University of Waikato, Private Bag 3105, Hamilton 3240, New Zealand

Cover photo:

Looking south over Lake Rerewhakaaitu from the slopes of Mount Tarawera, New Zealand. Tauhara is visible far right, along with Tongariro, Ngaruahoe and (faintly) Ruapehu.
https://commons.wikimedia.org/wiki/File:Lake_Rerewhakaaitu.jpg

Disclaimer:

Reviewed by: *Approved for release by*:

Grant Tempero — John Tyrell

University of Waikato — University of Waikato

Executive Summary

Lake Rerewhakaaitu in the Bay of Plenty Region of North Island, has one of the most intensively farmed lake catchments in New Zealand. Nitrate concentrations in two surface stream inflows to the lake show substantial and statistically significant increases, between 1995 and 2015, however, lake water quality has remained relatively stable. The lake is polymictic (i.e., it mixes frequently) and is partly perched, with an effective hydrological catchment of approximately 10% of the surface topographic catchment. We used the hydrodynamic-ecological model DYRESM-CAEDYM to examine the relationship between inflow quantity and quality, and lake water quality. A groundwater model (MODFLOW) provided groundwater discharge values from the hydrologically effective catchment, to the lake model (DYRESM-CAEDYM). The model successfully reproduced the magnitude and dynamics of field measurements, as evidenced by low statistical error. Based on a novel uncertainty analysis that allows for assessment of forcing factors that contribute to model error, a component of the statistical error was identified to be due to lake water level variations, which was attributed to ecological changes in the littoral (shallow-water) zone of the lake. The calibrated model was used with a set of scenarios to examine land use change within the effective hydrological catchment, as well as climate change. Establishment of the lake model was subject to several areas of substantial uncertainty, including derivation of stream inflows by statistical modelling (rather than direct observation), hydrological uncertainty with regard to drainage pathways in the lake catchment, and reliability of some nutrient measurements in the lake and streams. Nevertheless, the present model can be considered among the most sophisticated tools available with which to inform lake management decisions. Model results suggest that improved land management efforts within the wider topographic catchment will have only minor impacts on Lake Rerewhakaaitu water quality, but within the hydrologically effective catchment land use improvements to decrease losses of nitrogen and phosphorus to the lake will be important. Maintaining and/or enhancing the forested area within the hydrologically effective catchment and potentially retiring (to indigenous vegetation) some of the area, as well as maintaining the riparian buffer of the lake, will help to maintain water quality of Lake Rerewhakaaitu. The model predicted that a future warmer climate would likely increase the duration of temperature stratification in the water column, leading to more deoxygenation of bottom waters and a decline in water quality. Offsetting this with maintaining and enhancing vegetation in the riparian area and hydrologically effective catchment may help to offset these effects.

Acknowledgements

This study was supported by Bay of Plenty Regional Council (BOPRC) through the Chair in Lake Restoration at the University of Waikato, as well as the New Zealand Ministry of Business, Innovation and Employment (UOWX1503; Enhancing the health and resilience of New Zealand lakes). A number of people provided assistance and dedicated large amounts of time to this project: Andy Bruere (BOPRC), Chris Sutton (Rerewhakaaitu community), Paul Scholes (BOPRC) and John Paterson (BOPRC). The lake model DYRESM-CAEDYM was previously developed at the Centre for Water Research, The University of Western Australia.

Table of Contents

Executive Summary **3**
Acknowledgements **4**
Table of Contents **5**
Introduction **6**
Background 6
Study objectives 7
Methods **8**
Study site description 8
Trend analysis 8
Lake model description 10
Model input 10
General information 10
Hydrological information 12
Water quality information 13
Calculation of effective hydrological catchment 14
Analysis of effective forcing factor 15
Scenario analysis .... **Error! Bookmark not defined.**
Results **18**
Change in nutrient concentrations in Lake Rerewhakaaitu 18
Change in nutrient concentrations in stream discharges to Lake Rerewhakaaitu 19
Calibration and validation of hydrology and effective hydrological catchment of Lake Rerewhakaaitu 20
Calibration and validation of DYRESM-CAEDYM 23
Effective forcing factor 31
Scenario analysis 33
Discussion **39**
Conclusions **41**
References **42**

Introduction

Background

Mitigation of diffuse pollution is an ongoing challenge as human populations increase and food preferences switch towards higher energy sources, requiring agricultural production to increase to meet this demand (Collins and McGonigle 2008, D'Arcy and Frost 2001, Hamilton et al. 2016a). Hydrologically, diffuse pollution is associated with various transport pathways which are often uncertain and not clearly defined (Howard-Williams et al. 2010). For this reason, and because land use controls are more difficult to implement in a unified way across multiple land owners and kaitiaki, diffuse pollution has not been controlled as effectively as point source discharges of contaminants to surface and ground waters (D'Arcy and Frost 2001, Heathwaite et al. 2005). Globally, agriculture is the most important contributor to diffuse pollution, particularly as point source controls on nutrients have taken effect across the developed world and agricultural intensification has occurred through several mechanisms, notably increased use of fertilizers and greater stock densities and manure production (D'Arcy and Frost 2001, Gömann et al. 2005, Wang and Yang 2008).

Pastoral agriculture is the single largest land use category in New Zealand and occupies approximately 40% of the nation’s total land area (Davies-Colley 2013). Given the large area of pastoral farming, diffuse pollution has been reported to have a significant impact on water quality in New Zealand as a result of enrichment by nitrogen and phosphorus leading to eutrophication (Davies-Colley 2013, Howard-Williams et al. 2010). In addition, there has been very rapid intensification of pastoral land use over the past two decades (PCE 2004, PMCSA 2017). Thus there has been a progression from not only managing lakes for conservation purposes (e.g. Vant et al. 1987), to restoring them using controls on external and internal loads (e.g. Hamilton et al. 2016b, Özkundakci et al. 2013, Smith et al. 2016).

Deterministic models provide a means of developing decision support systems for lake management and restoration. These models can be valuable tools for quantifying the relative contributions of external and internal nutrient loads (Burger et al. 2008, Özkundakci et al. 2013) including considerations of resilience of the lake ecosystem due to lags in the response of the bottom sediments to changes in catchment nutrient loads (Dada and Hamilton 2016). These models have various degrees of complexity and parameterization which reflect the prevailing epistemology of the processes that are represented, the questions being asked by the modellers, and the quality and availability of input data. Uncertainty analysis following calibration and validation of the model helps to quantify some of the inherent model uncertainties (Cho et al. 2016) and can ultimately improve understanding of the complex responses of environmental systems as well as providing greater confidence to assist with the implementation of management plans (Ascough Ii et al. 2008).

Nutrients in groundwater inflows can be a significant source of diffuse pollution to the standing waters of lakes (Gömann et al. 2005, Kim et al. 2007). Nutrients in groundwater combine with those in surface water inflows and may lead to eutrophication of lakes, which is reflected in harmful algal blooms, deoxygenation, and loss of ecosystem services and amenity value (Collins and McGonigle 2008, Liu et al. 2005, Wang and Yang 2008). Several models are available to assess the fate and transport of nutrients to lakes arising from groundwater and surface water inputs (e.g., Shoemaker et al. 2005). Many catchment and lake models operate with reduced dimensionality, eliminating one or more of the relatively homogeneous or well-mixed dimensional constituents in order to reduce computational times and demonstrate inter-annual variability expected with most catchment nutrient mitigation strategies. At the catchment scale they include the groundwater model MODFLOW (Yang et al. 2017b), the surface hydrological model SWAT (Me et al. 2015) or other GIS-based tools (Yang et al. 2017a). For lakes they include one-dimensional models such as DYRESM-CAEDYM (Burger et al. 2008).

Lake Rerewhakaaitu is a moderate-sized (area = 5.1 km^2, mean depth = 7 m, max depth = 15 m), polymictic lake. It is one of several lakes of volcanic origin in the Rotorua region, known collectively as Te Arawa lakes. The volcanic soils of Lake Rerewhakaaitu have high porosity and are known to be highly retentive of phosphorus (Fish 1978). The topographic catchment is of moderate size (53 km^2; Reeves et al. 2008) and highly developed for intensive pastoral agriculture (70%; Reeves et al. 2008), which belies the relatively moderate nutrient status (mesotrophic) of the lake (Burns et al. 2009, McIntosh et al. 2001). The reason for this may be related to lake water levels which are higher than those within most of the catchment area, thus categorising the lake as at least partially perched (White et al. 2003). Inputs from the elevated topographic catchment (i.e., where the surface land contour is above lake water level) may arise only from a relatively small area within the topographic catchment (White et al. 2003, 2015). Most studies of perched lakes have focused on monitoring habitat distributions (Armiento et al. 2015, Chikita et al. 2004) or hydrodynamics (Ayenew and Tilahun 2008, Baiocchi et al. 2006) and few have sought to use a model to relate the area and location of the inflows to the water quality of the lake. We simulated catchment hydrology and estimated nutrient loads to Lake Rerewhakaaitu, and linked these outputs to a coupled hydrodynamic−water quality model of the lake.

Study objectives

Coupled output from a groundwater model (MODFLOW) and a lake model (DYRESM-CAEDYM) was employed in order to understand why widespread land use intensification in the surface topographic catchment of Lake Rerewhakaaitu has not strongly impacted lake water quality. We hypothesized that the small surface topographic catchment of Lake Rerewhakaaitu may limit the extent to which land management activities impact lake water quality, and that direct effects of climate change on lake mixing processes could strongly offset benefits from good land management. We tested this hypothesis by examining the hydrological catchment land use and quantifying expected nutrient yields. We also ran scenarios of lake water quality changes using different combinations of catchment nutrient loading and possible climate changes. Additionally, a novel uncertainty analysis that allows for assessment of forcing factors was performed for the lake model to understand whether error between observed and simulated data was related to forcing factors not included in the model inputs.

Methods

Study site description

Lake Rerewhakaaitu (36°18'S, 176°30'E) is a shallow, polymictic lake in the Bay of Plenty Region, North Island, New Zealand. The lake was formed in a volcanic caldera from the Kaharoa eruption of 0.7 ka (Viner 1987). It is located on the southern slopes of Mount Tarawera and 26 km south-east of Lake Rotorua. The lake surface is approximately 435 m above mean sea level. The lake has a main basin and a small sidearm crater (area = 0.1 km^2, mean depth = 15 m, max depth = 31 m) which sometimes connects to the main basin at high water levels (Chapman et al. 1981). Only the main basin was simulated in this study.

The area of the surface topographic catchment is 51.83 km^2 based on a New Zealand 8-m Digital Elevation Model (DEM) (LINZ 2012a). The catchment is mostly flat to moderately rolling with elevations 420 to 530 m above mean sea level (masl). Current catchment land use is mostly high producing grassland, primarily dairy farming (c. 50% of the total catchment) and a small amount of drystock farming (Fig. 1), as well as substantial areas of native and exotic vegetation (Figure 1).

Trend analysis

A Mann-Kendall test was used to analyse a monotonic trend of nutrient concentrations in the lake from 2000 to 2016 and in the streams from 1995 to 2016 using the R Kendall package with R version 3.3.1 (R Development Core Team 2013). A positive (negative) Z value means an increasing (decreasing) trend for which statistical significance was set at $p < 0.05$. Linear regression or linear regression with logarithmic transformation models were performed in Matlab for statistically significant Mann-Kendall tests.

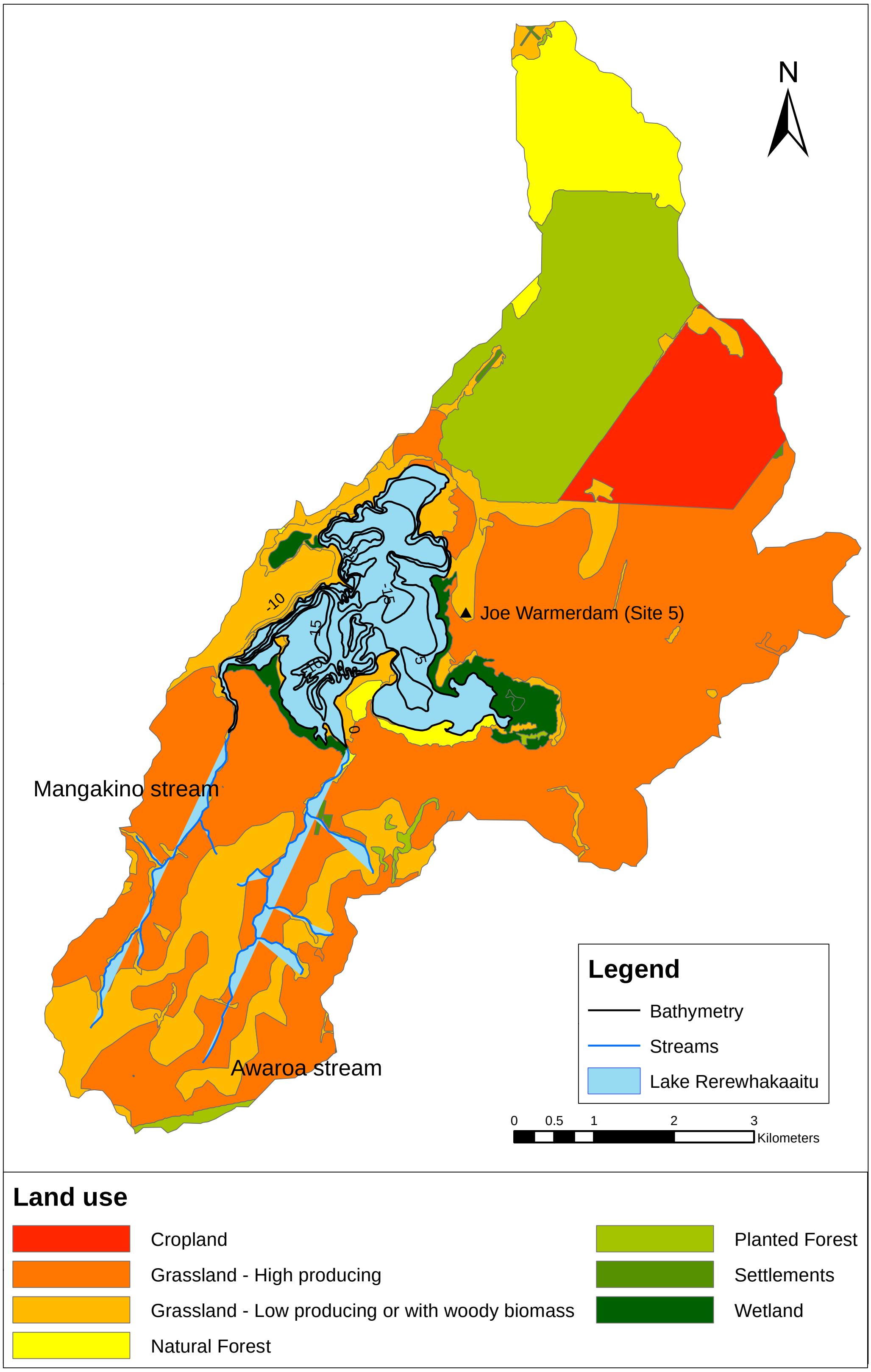

Figure 1. Current land use by simplified classification based on surface catchment and bathymetry of Lake Rerewhakaaitu with Mangakino and Awaroa Stream.

Lake model description

A process-based hydrodynamic-biogeochemical lake model (DYRESM-CAEDYM) was used for simulation of hydrodynamics and water quality, respectively. Both models were originally developed at the Centre for Water Research, The University of Western Australia. DYRESM (DYnamic RESErvoir Simulation Model V.3.0), is a one-dimensional hydrodynamic model which suitable for long-term (multi-year) simulations (Ziemińska-Stolarska and Skrzypski 2012). It was used to simulate the vertical distribution of temperature and the vertical mixing and transport of water. CAEDYM (Computational Aquatic Ecosystem DYnamics Model), is an aquatic ecological model, and was used to simulate dissolved oxygen (DO) concentration, nutrient concentrations such as nitrogen (N) and phosphorus (P), inorganic suspended solids (SS) concentration, and phytoplankton biomass. Model equations are described in detail in several publications (e.g., Bruce et al. 2006, Burger et al. 2008, Hamilton and Schladow 1997, Schladow and Hamilton 1997).

Model inputs

General information

Calibration and validation periods for lake water temperature and DO concentration were July 2015-May 2016 and September 1992-May 2016, respectively. High frequency environmental data, obtained from a water column profiling monitoring buoy in the central part of the lake, were used for calibration of temperature and oxygen dynamics, and monthly water quality observations obtained from Bay of Plenty Regional Council (BOPRC), were used for calibration and validation of the biogeochmical model. Calibration and validation periods for nutrients, SS, phytoplankton biomass (chlorophyll *a*), and Secchi depth were September 2013-May 2016 and September 1992-August 2013, respectively. The monthly data obtained from BOPRC were used for model calibration and validation. Lake water level monitored by National Institute of Water and Atmospheric Research (NIWA) was used to achieve a lake water balance. Model parameters were adjusted manually using a trial and error approach to match the model simulations with observed data, with statistical metrics used to quantify goodness of fit. Statistical comparison of model simulations against observed data was performed using root mean square error (RMSE), normalised RMSE (NRMSE), and coefficient of determination (R^2) for calibration and validation.

Bathymetry of the lake was quantified using two maps; 'Lake Rerewhakaaitu, Provisional Bathymetry' (Irwin 1970) for 5 m contours, and 'BF38, Topo50 Maps' (LINZ 2012b) for the most recent lake shape, updated December 2014. Daily meteorological data for model input were obtained from the Meteorological Service of New Zealand for the Rotorua Airport weather station which is located 26 km northwest of the lake. The data included air temperature (°C), short wavelength radiation (W m^{-2}), cloud cover (fraction of whole sky), vapour pressure (hPa), and wind speed (m s^{-1}), as shown in Fig. 2. Vapour pressure was estimated based on wet and dry bulb temperature or relative humidity and air temperature (Wunderlich 1972), and cloud cover was estimated by fitting a seasonal sinusoidal curve to the maximum and minimum observed daily shortwave radiation values across the entire simulation period (Jones et al. 2012). Precipitation was adjusted to a volumetric input using lake surface area, which was variable according to lake water levels, and was included in daily inflow data, as this allowed for inclusion of atmospheric deposition of N and P.

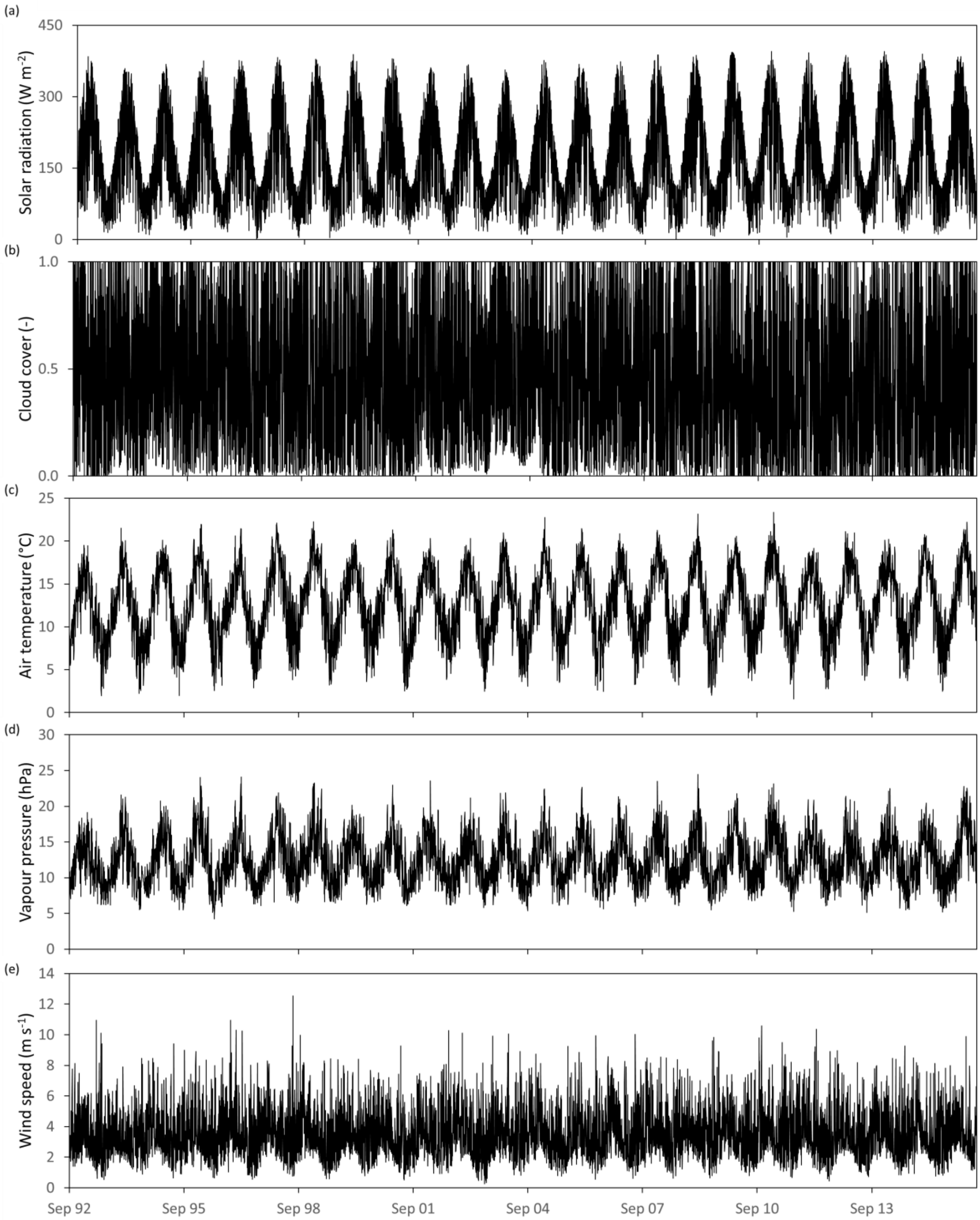

Figure 2. Meteorological input data for (a) solar radiation, (b) cloudy cover, (c) air temperature, (d) vapour pressure, and (e) wind speed.

Hydrological information

Mangakino Stream is a permanent inflow to the lake, however, the flow is only measured at monthly intervals. Daily inflow to the model for Mangakino Stream was estimated using a correlation of its discharge against Ngongotaha Stream, a continuous discharge to Lake Rotorua (McIntosh 2012). The fraction of variation explained for this relationship was closer than a number of other streams which were tested as alternatives to Ngongotaha (Fig. 3(a)). A second inflow to Rerewhakaaitu, Awaroa Stream flows only during extreme rainfall events and is otherwise dry (McIntosh 2012). The flow rate is measured occasionally during flooding events. Daily discharge of Awaroa Stream was estimated using a correlation with the flow of Mangakino Stream (Fig. 3(b)). Residual inflow comprised groundwater inflow and diffuse surface runoff.

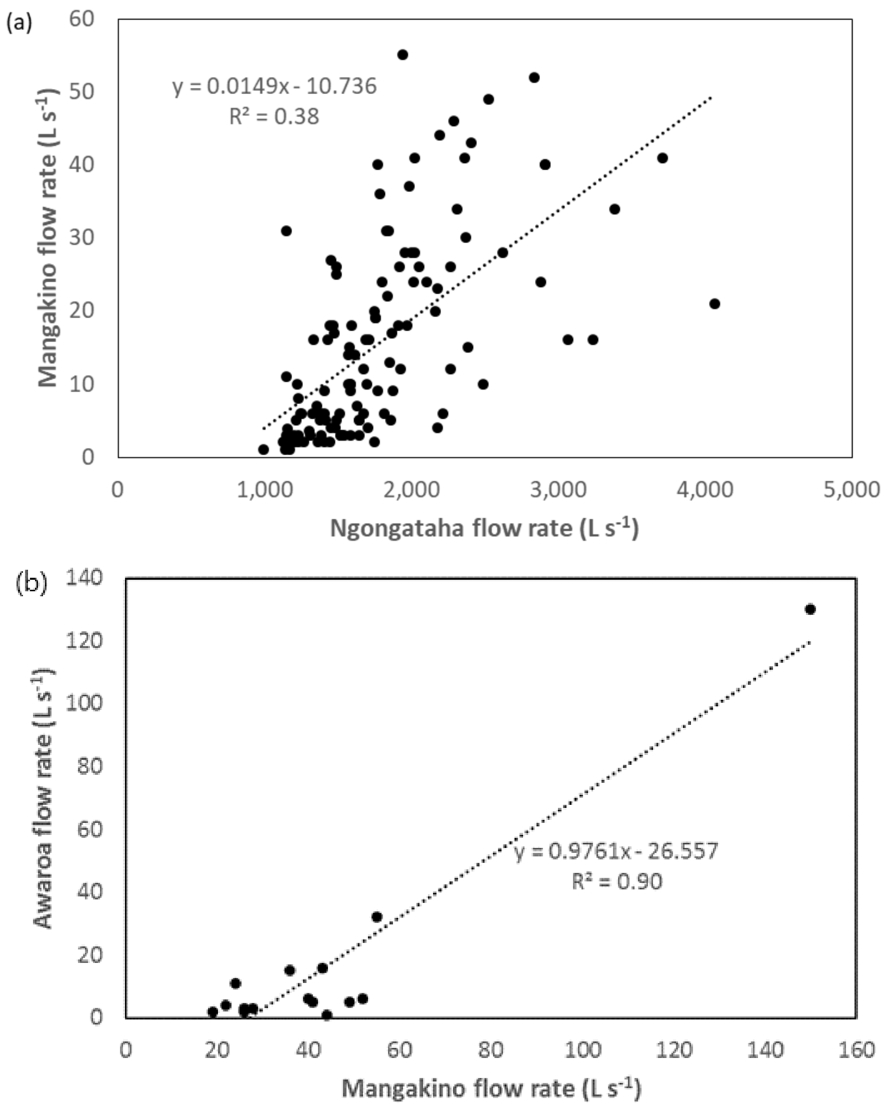

Figure 3. Relationship between (a) Ngongataha Stream flow rate and Mangakino Stream flow rate and (b) between Mangakino Stream flow rate and Awaroa Stream flow rate.

Outflow from Lake Rerewhakaaitu was assumed to include only groundwater and evaporation because the lake outflow channel remains almost continuously dry (McIntosh et al. 2001, Reeves et al. 2008). Annual average groundwater outflow was previously reported as part of a water budget for the greater Tarawera catchment, White et al. (2015) used the software GMS 10.0 with a conceptual model approach to build finite difference MODFLOW and MT3DMS models from vector-based solid geologic models and GIS data. MODFLOW-2005 in conjunction with MT3DMS v5.3 was used to simulate groundwater flow, and MODFLOW-NWT was additionally used to calibrate MODFLOW-2005 as it converges more reliably on hilly topography where many dry cells are anticipated. Simulations from the two versions of MODFLOW were compared to ensure they produced similar groundwater flows.

Daily residual inflow and daily groundwater outflow were calculated from a water balance for the lake which included all of the previously stated inflows and outflows, as well as the volume associated with changes in daily lake water level. This was an interactive fitting procedure based on matching observed and simulated daily water levels. Preliminary simulated lake water level was obtained using constant outflow, which is the reported average annual value for groundwater (White et al. 2015), and inflows with zero residual inflow. Using the preliminary simulated lake water level and observed lake water level, the volume for daily residual inflow and daily variation of groundwater outflow was calculated based on the multiplication of the difference between those lake water levels and the lake surface area when lake water level is the median value of those water levels. This calculation was iterated several times to match the simulated lake water level to observed lake water level. Daily residual inflow and daily groundwater outflow were managed simultaneously to match an average annual value of groundwater outflow. Finally, daily residual inflow and daily groundwater outflow were obtained using three-day averages, to provide continuity of flow and to reduce daily inflow variation as an artefact of short-term fluctuations in observed lake water level (e.g., due to wind set-up).

Water quality information

Daily temperature of rainfall prescribed in the inflow file was assumed to be same as the air temperature on that day. Daily water temperatures of the two streams were estimated using a nonlinear regression model which is an S-shaped logistic function with four parameters, associated with the estimated maximum and minimum water temperatures, the steepest slope of the function and the air temperature at the point of inflection (Mohseni et al. 1998). Daily water temperature for residual inflow was estimated based on the ratio as shown in Table 1. This was obtained using observed Mangakino Stream and ground water temperatures measured at Site 5 located at Ash Pit Road to the east of Lake Rerewhakaaitu as shown in Fig. 1 (Rose et al. 2012). Daily water temperature for residual inflow was therefore obtained as the product of the ratio (0.94) and daily water temperature of the Mangakino Stream.

The DO concentration in rainfall was estimated from assuming saturation of DO calculated using air temperature. Similarly, daily DO concentrations for streams were estimated from the stream temperature and assuming saturation of DO. Daily DO concentration for residual inflow was calculated using the ratio in Table 1 and daily DO concentration for Mangakino Stream.

Daily nutrient data for precipitation were taken to be 1.5 kg N ha^{-1} yr^{-1} (Parfitt et al. 2008a) and 0.2 kg P ha^{-1} yr^{-1} (Parfitt et al. 2008b). Organic nutrients, including dissolved and particulate organic phosphorus (DOP and POP) and dissolved and particulate organic nitrogen (DON and PON) in precipitation, were set to zero. Daily nutrient data for the two streams were generated by the interpolation between the observed data or from averaged values for 24 years where measurement frequency was less than monthly. Daily SS concentrations for Mangakino Stream were estimated using a relationship between SS concentrations and flow rates measured monthly, and daily SS concentrations for the Awaroa Stream were taken to be an averaged value of the observed data due to infrequent measurements. The ratio of dissolved and particulate organic nutrients for streams was followed based on the reported value of dissolved and total phosphorus for Mangakino Stream (McDowell and Hawke 2006). Daily water quality data for the residual flow were estimated using the product of this ratio and daily water quality data for Mangakino Stream.

Table 1. Observed data for Mangakino Stream and groundwater stations in the Lake Rerewhakaaitu catchment. Groundwater samples are averages from various depths at Site 5. The 'Average' is the ratio of groundwater samples values to Mangakino stream samples. The 'Ratio' used to estimate daily temperature and concentrations of nutrients in groundwater based on daily value for Mangakino Stream.

Location	Date	Reference	Variables						
			Temp (°C)	DO ($g\ m^{-3}$)	NH_4-N ($g\ m^{-3}$)	NO_3-N ($g\ m^{-3}$)	DON/PON (-)	PO_4-P ($g\ m^{-3}$)	DOP/POP (-)
Mangakino Stream	2011-10-04	BOPRC	14.1	8.71	0.138	3.51	0.582	0.085	0.087
JW-Deep1	2011-09-29	Rose et al. (2012)	13.2	2.55	0.24	0.005	0.055	0.032	0.103
JW-Deep2	2011-08-09		13.2	0.75	0.36	0.025	0.285	0.015	0.062
JW-Shallow1	2011-09-27		13.4	2.87	0.85	0.84	0.28	0.015	0
JW-Shallow2	2011-09-27		13.4	2.87	0.86	0.83	0.26	0.014	0
Average			13.3	2.260	0.578	0.425	0.220	0.019	0.041
Ratio			0.94	0.26	4.18	0.12	0.38	0.22	0.47

JW-Deep1: Well depth 100 m BGL / JW-Deep2: Well depth 60 m BGL / JW-Shallow1, 2: Well depth 19 m BGL

Calculation of effective hydrological catchment

Median annual rainfall was estimated by GIS using a nationwide map of long-term rainfall measurements at individual climate stations (Tait et al. 2006), adjusted for the period 1960-2006 and interpolated throughout New Zealand by NIWA. Median annual evapotranspiration was also estimated over the lake catchments by GIS using evapotranspiration values from the land surface derived from a national-scale map developed by NIWA, and averaged for the period 1960-2006 without specific consideration of land use, land cover, soil type or groundwater recharge (Woods et al. 2006). It was assumed that rainfall on land, after removal of evapotranspiration, contributed to groundwater, with no loss due to water intake for human and animal consumption, and the coefficient of permeability for all area was assumed the same. A virtual catchment was assumed first, then the difference between median annual rainfall and median annual evapotranspiration in a 500 m^2 grid was calculated for the virtual catchment. The averaged value for all grids in the virtual catchment was multiplied by the area of the virtual catchment to obtain an annual median flow rate. The calculated annual median flow rate for each virtual catchment was compared with an average flow rate of each inflow for 24 years. If the calculated annual average flow rate was larger (smaller) than the average flow rate of each inflow for 24 years, the virtual catchment area was assumed to be smaller (larger) than the previous virtual catchment area. The effective hydrological catchment was then determined by repeated iteration, corresponding to when there was a match of the calculated annual averaged flow rate between the virtual catchment the inflows.

Analysis of effective forcing factor

Errors between daily model simulation outputs and observed data were regressed against forcing factors such as daily lake water level and daily meteorological data in order to test whether changes in specific forcing factors contributed disproportionately to errors in the model output, i.e., suggesting that they were not adequately captured in the model representation of that factor.

Model scenario simulations

Six scenarios indicative of varying hypothetical future catchment land use and/or climate were simulated for the period 2090-2099 (Table 2). The scenarios were classified into two groups based on stable or changing future climate, whereby meteorological data for the baseline period of 2003-2012 were perturbed to represent likely climate change conditions.

The Land Use Classification (LUC) from the New Zealand Ministry for the Environment (LUCAS 2016) was simplified to six classifications for scenario analysis, including: 1) high producing grassland, 2) low producing grassland or grassland with woody biomass, 3) natural forest, 4) planted forest, 5) settlements (combination of settlements and other (e.g., bare rock, quarry)), and 6) wetlands (combination of wetlands and lakes) (White et al. 2015). Nitrogen and phosphorus loading from the lake catchment was derived according to the simplified land use and assumed areal nutrient export coefficients and is shown in Table 3.

Land use scenarios included baseline catchment land use as used for model calibration and validation (Current), an increase of nutrient concentration in streams (Stream), and intensified land use (High-production). The 'Stream' scenario represented changes in nutrient concentrations of the two streams by extrapolating the observed long-term trend. The 'high-production' scenario assumed that all current land use changed to high producing grassland (e.g., dairy production) within the effective hydrological catchment area.

Climate change scenarios included a completely forested catchment with climate change (Forest_CC), current land use with climate change (Current_CC), and intensified land use and increase of nutrient concentration in streams with climate change (High-production_Stream_CC). The 'Forest_CC' scenario represents the change of all high producing grassland area to planted forest, i.e., catchment management resulting in reduced nutrient concentrations in the two streams and residual inflow, but under a future climate. Conversely, 'High-production_Stream_CC' scenario represents the combination of climate change, 'Stream' scenario, and 'High-production' scenario, i.e., the most extreme scenario. Future climate was produced for 2090-2099 using change factors which were estimated using SimCLIM 2013 (Yin et al. 2013). This model is based on outputs from the Intergovernmental Panel on Climate Change Fifth Assessment Report (IPCC AR5) All data were processed by a pattern scaling method, and then were regridded to a common 720 x 360 grid using a bilinear interpolation method which was applied to interpolate the data from General Circulation Models (GCMs) original resolution. The most basic spatial dataset (baseline and future) is run at the global scale of 0.5° x 0.5° resolution. Twenty-two GCMs were selected to generate which included air temperature, precipitation, solar radiation, relative humidity, and wind speed variables (Fig. 4). Representative concentration pathway 8.5 with radiative forcing of 8.5 W m^{-2} in 2100, was selected as an extreme prediction case for climate change.

Table 2. Configuration of six modelled scenarios, corresponding to current land use (Current), land use intensity with current was increase of nutrient concentration in streams (Stream), intensified land use scenario (High-production), all forest with climate change scenario (Forest_CC), current land use with climate change scenario (Current_CC), and intensified land use and increase of nutrient concentration in streams with climate change (High-production_Stream_CC).

Scenario	Acronym	Change of land use	Change in streams	Climate inputs
Land use intensification scenarios	Current	Baseline	Baseline	2003-2012
	Stream	Baseline	Predicted trajectory	2003-2012
	High-production	Intensification	Predicted trajectory	2003-2012
Climate change scenarios	Forest_CC	Afforestation	Baseline	2090-2099
	Current_CC	Baseline	Baseline	2090-2099
	High-production_Stream_CC	Intensification	Predicted trajectory	2090-2099

Inflows, outflow and lake water level in climate change scenarios were estimated using a linear regression model and iterative calculation with Excel-VBA. For inflows it was assumed that the ratio between precipitation and evapotranspiration would not be changed in the future, so future inflows were calculated by the product of the change factor for future precipitation and current flow for 2003-2012. Precipitation on the lake is a function of lake surface area, so the future lake water level was estimated based on the linear regression between the difference of daily water level and sum of inflows as shown in Fig. 5. After several iterative calculations to achieve stable simulated water level, the final future water level was observed as shown in Fig. 6. Future outflow was adjusted using this future lake water level.

Table 3. Nitrogen and phosphorus loading from Lake Rerewhakaaitu catchment according to land use (McIntosh 2012; Hamilton 2014). Settlements are set to zero due to interception by wastewater systems.

	Nitrogen loading (kg ha^{-1} yr^{-1})	Phosphorus loading (kg ha^{-1} yr^{-1})
Grassland - High producing	31	1.1
Grassland - Low producing or with woody biomass	3.67	0.12
Wetland	0	0
Natural Forest	3.67	0.12
Planted Forest	2.81	0.18
Settlements	0	0

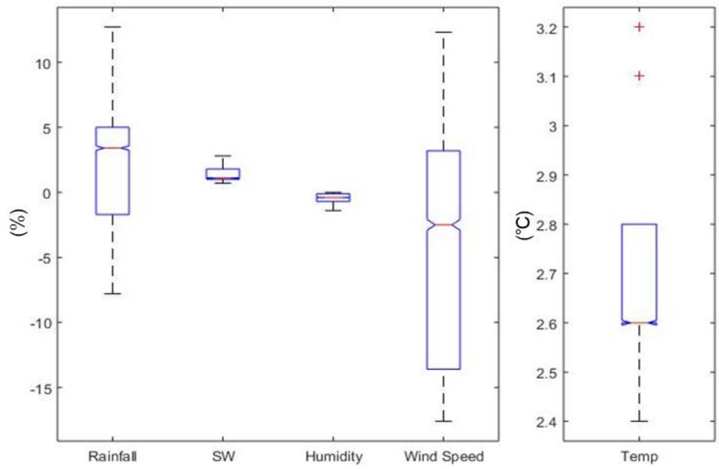

Figure 4. Variation based on percentage or absolute value of monthly meteorological data for climate change scenarios based on Intergovernmental Panel on Climate Change Fifth Assessment Report (IPCC AR5). From left to right: rainfall, shortwave radiation (SW), humidity, wind speed, and air temperature (Temp).

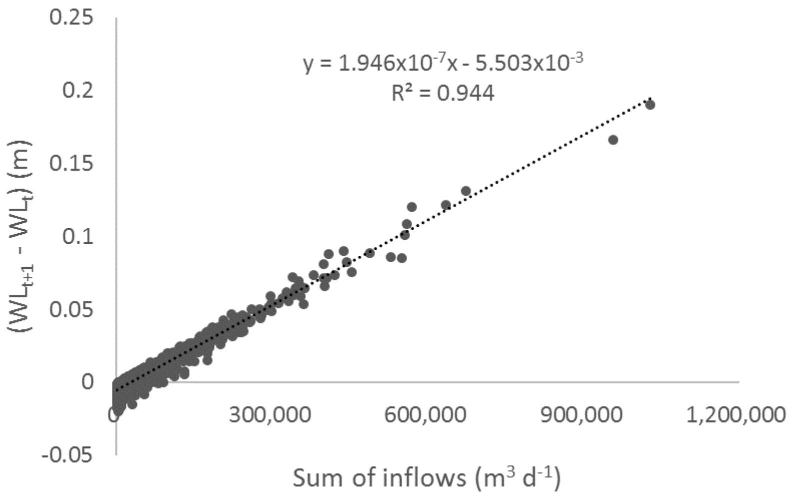

Figure 5. Linear regression model between the difference of daily water level ($WL_{t+1} – WL_t$) and sum of inflows including two stream flows, groundwater and runoff.

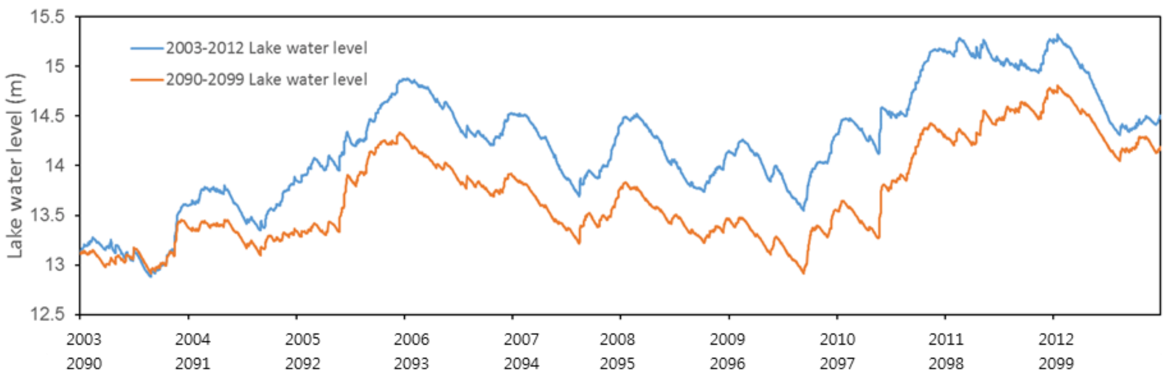

Figure 6. Present (2003-2012) and estimated future (2090-2099) lake water level calculated by iteration using Excel-VBA.

Results

Change in nutrient concentrations in Lake Rerewhakaaitu

Nutrient concentrations in Lake Rerewhakaaitu were examined for changes over the study period using a Mann-Kendall test and linear regression. The results of the Mann-Kendall test and linear regression are shown in Fig. 7 and Table 4 using monitoring data from BOPRC for 24 years. Total phosphorus and nitrate-N concentrations showed an increasing trend with a positive Z-value and $p < 0.05$. For these two nutrients where significant trends were identified, linear regressions were fit to the time series to describe the rate of increase. For total phosphorus this increase was 2.21×10^{-4} g m^{-3} yr^{-1} ($p = 9.37 \times 10^{-10}$) and for nitrate-N it was 1.97×10^{-4} g m^{-3} yr^{-1} ($p = 0.035$).

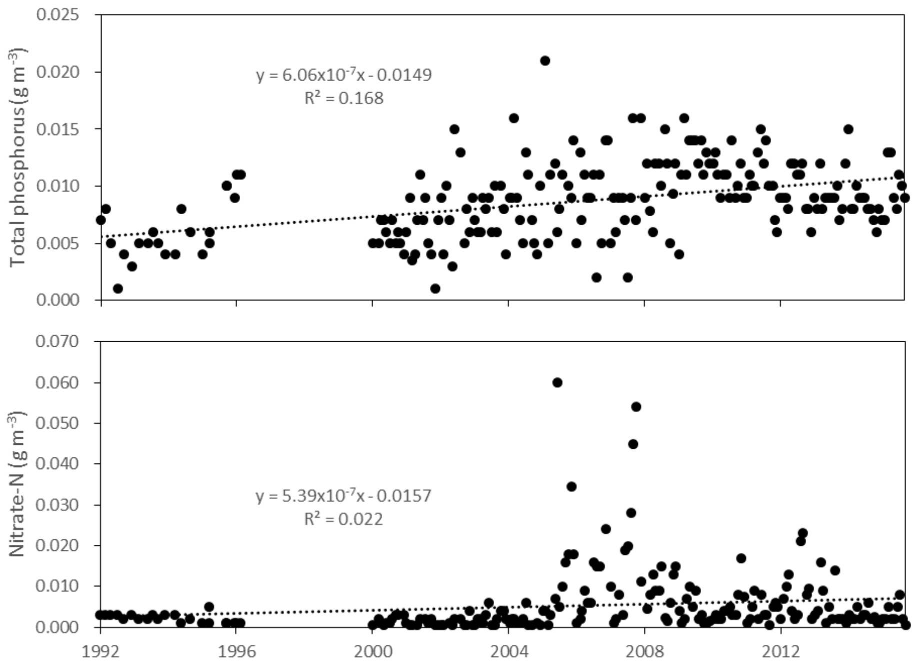

Figure 7. Time trends for total phosphorus (p = 9.37 x 10-10) and nitrate-N (p = 0.035) in Lake Rerewhakaaitu based on linear regression versus time.

Table 4. Results of Mann-Kendall test and linear regression analysis for concentrations of total nitrogen (TN), ammonium-N (NH_4-N), nitrate-N (NO_3-N), total phosphorus (TP), phosphate-P (PO_4-P), suspended solids (SS), and total chlorophyll-*a* (TChl-*a*), and Secchi depth for lake (1992-2016) and streams (1995-2016). Bold inidcates p-value < 0.05 (95 % confidence).

Variable	Lake Rerewhakaaitu				Mangakino stream				Awaroa stream			
	Mann-Kendall		Linear regression		Mann-Kendall		Linear regression*		Mann-Kendall		Linear regression*	
	Z	p-value	R^2	p-value	Z	p-value	R^2	p-value	Z	p-value	R^2	p-value
TN	-1.5	0.137	-	-	9.5	**2.22×10^{-16}**	0.541	**5.46×10^{-27}**	0.1	0.928	-	-
NH_4-N	-0.2	0.815	-	-	0.4	0.653	-	-	-0.5	0.650	-	-
NO_3-N	3.7	**1.90×10^{-4}**	0.022	**0.035**	11	**2.22×10^{-16}**	0.709	**4.35×10^{-43}**	2.1	**0.032**	0.353	**4.50×10^{-3}**
TP	5.7	**1.53×10^{-8}**	0.168	**9.37×10^{-10}**	6.8	**9.34×10^{-12}**	0.032	**0.027**	-0.6	0.526	-	-
PO_4-P	2.3	0.020	-	-	4.6	**4.24×10^{-6}**	0.081	**3.13×10^{-4}**	-0.5	0.603	-	-
SS	1.6	0.114	-	-	-4.1	**3.68×10^{-5}**	2.80×10^{-3}	0.524	-0.2	0.846	-	-
TChl-*a*	1.1	0.266	-	-	-	-	-	-	-	-	-	-
Secchi depth	0.3	0.740	-	-	-	-	-	-	-	-	-	-

* Linear regression with logarithmic transformation (Linear-log model)

Change in nutrient concentrations in stream discharges to Lake Rerewhakaaitu

Nutrient concentrations in the two surface inflows to Lake Rerewhakaaitu (Mangakino and Awaroa Streams) were examined for changes over the study period using a Mann-Kendall test and linear regression with logarithmic transformation (Fig. 8(a)-(c) and Table 4). In the Awaroa Stream, only nitrate-N showed a significant monotonic upward trend, while in the Mangakino Stream total nitrogen, nitrate-N, total phosphorus, phosphate-P, and suspended solids showed a significant monotonic upward trend ($p < 0.05$). Where significant trends were identified, linear-log regressions were fitted to describe the rate of increase in concentrations. The regression model shown in Fig. 8(a)-(c) was used to calculate future nitrate-N and phosphate-P concentrations in Mangakino Stream and nitrate-N concentration in Awaroa Stream for the scenarios, by extrapolation 2090 to 2099.

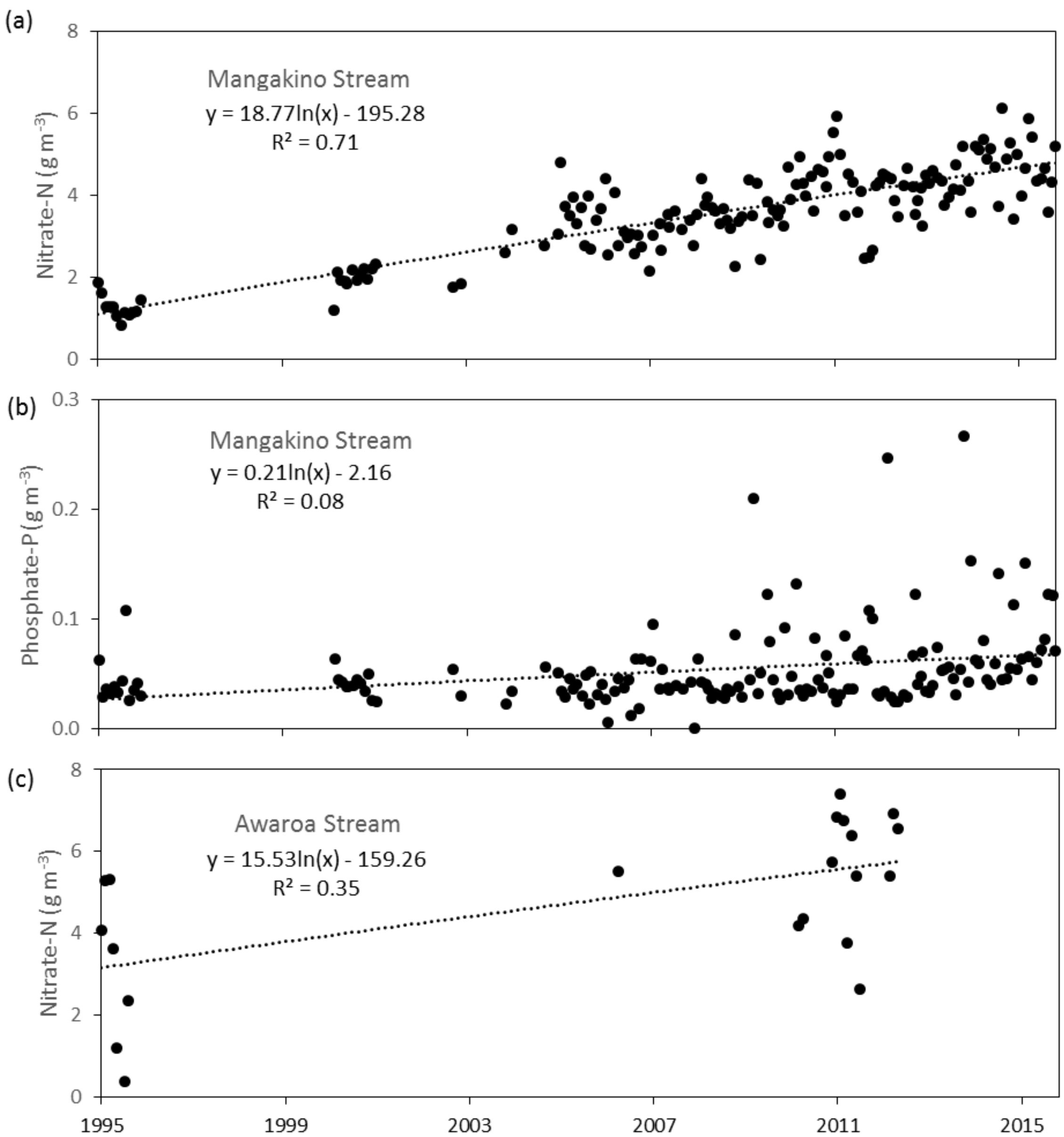

Figure 8. Time trends for (a) nitrate-N (p-value = 4.35×10^{-43}) and (b) phosphate-P concentrations (p-value = 3.13×10^{-4}) in Mangakino Stream and (c) nitrate-N concentration (p-value = 4.50×10^{-3}) in Awaroa Stream based on log-transformed concentrations versus time.

Calibration and validation of hydrology and effective hydrological catchment

Observed and simulated lake water levels are shown in Fig. 9. Comparison of observed and simulated water levels gave RMSE, NRMSE, and R^2 values of 0.02 m, 0.8%, and 0.99, respectively. These errors occurred due to rounding of the fluctuation of daily residual inflow and daily groundwater outflow generated from the uncertainty of lake water level measurement. The water budget for inflow and outflow of Lake Rerewhakaaitu is shown in Table 5. Inflows other than residual inflow were averaged values for 24 years, and residual inflow was estimated based on the water balance. Groundwater outflow was set to the annual average value given in White et al. (2015). The sum of average inflow and outflow (including precipitation and evaporation from the lake) for the whole simulation period (24 y), was identical (317 L s^{-1}), because there was no change of lake volume (water level) between the start date (1 September 1992) and end date (31 May 2016). The water balance indicated that rainfall and groundwater inflows account for the most of the total inflow volume to the lake.

The surface topographic catchment and effective hydrological catchment for Lake Rerewhakaaitu are shown in Fig. 10. Among sources of inflow to the lake, groundwater was the largest. Groundwater inflow catchment was estimated based on the reported groundwater level in White et al. (2015) as shown in Fig. 11 and surface topography. The groundwater levels are higher than the lake water level only in the north-east area of the catchment and the groundwater inflow catchment was placed in this area.

The total area of effective hydrological catchment based on the water balance was approximately one-tenth of the surface catchment area of 51.83 km^2. The predominant land use in the effective hydrological catchment comprised planted forest (44 %), high producing grassland (27 %) and low producing grassland (25 %). The dominant land use in the groundwater catchment was planted forest, while for the stream catchments it was high producing grassland.

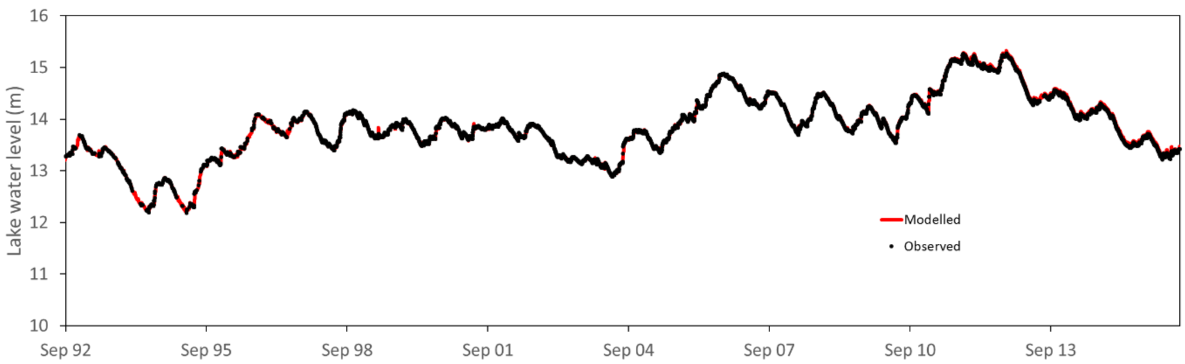

Figure 9. Model simulations (red line) and observed data (dots) for lake water level for the period of 1992-2016.

Table 5. Water balance and effective hydrological catchment of Lake Rerewhakaaitu by area and by percentage.

		Flow rate	Effective hydrological catchment area
Inflow	Precipitation	210 L s^{-1} (66 %)	-
	Groundwater inflow	82 L s^{-1} (26 %),	3.74 km^2 (73 %)
	Runoff	8 L s^{-1} (2 %)	0.44 km^2 (9 %)
	Mangakino stream	15 L s^{-1} (5 %)	0.82 km^2 (16 %)
	Awaroa stream	2 L s^{-1} (1 %)	0.10 km^2 (2 %)
Outflow	Groundwater outflow	192 L s^{-1} (61 %)	-
	Evaporation	125 L s^{-1} (39 %)	-
	Sum of inflow/outflow	317 L s^{-1} (100 %)	Sum of effective hydrological catchment area 5.10 km^2

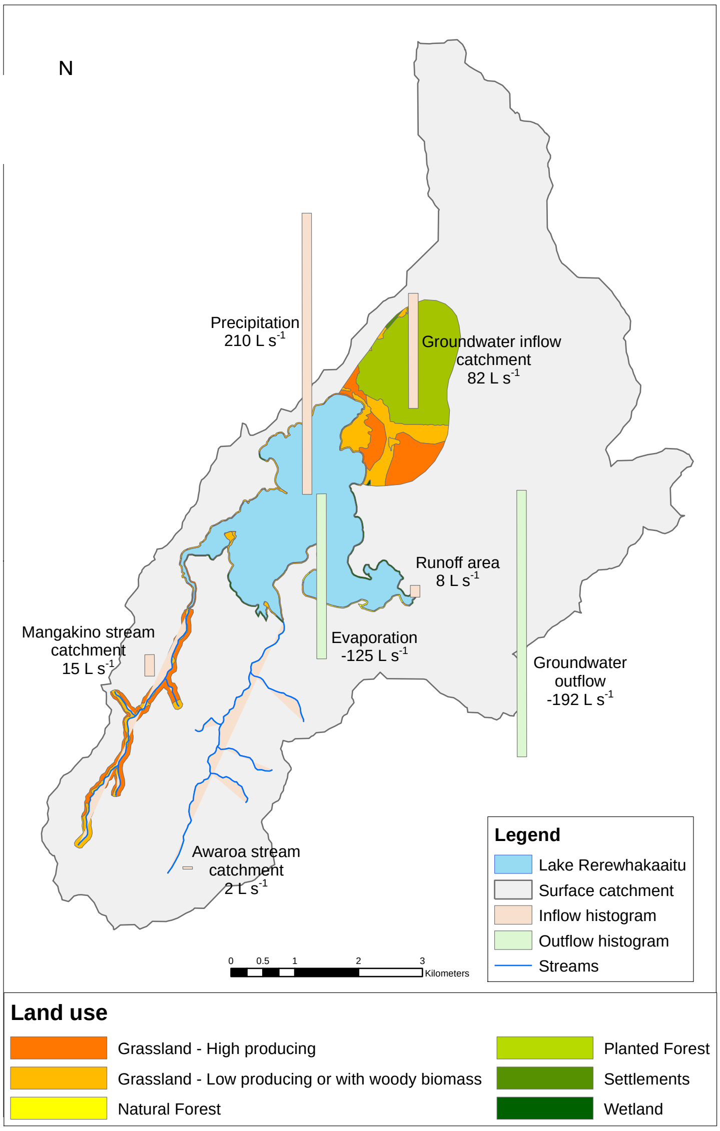

Figure 10. Map of Lake Rerewhakaaitu showing topographic and effective hydrological catchments. Histograms represent water entering (positive values) or leaving (negative values) the lake, respectively. Current land use is shown in the effective hydrological catchment.

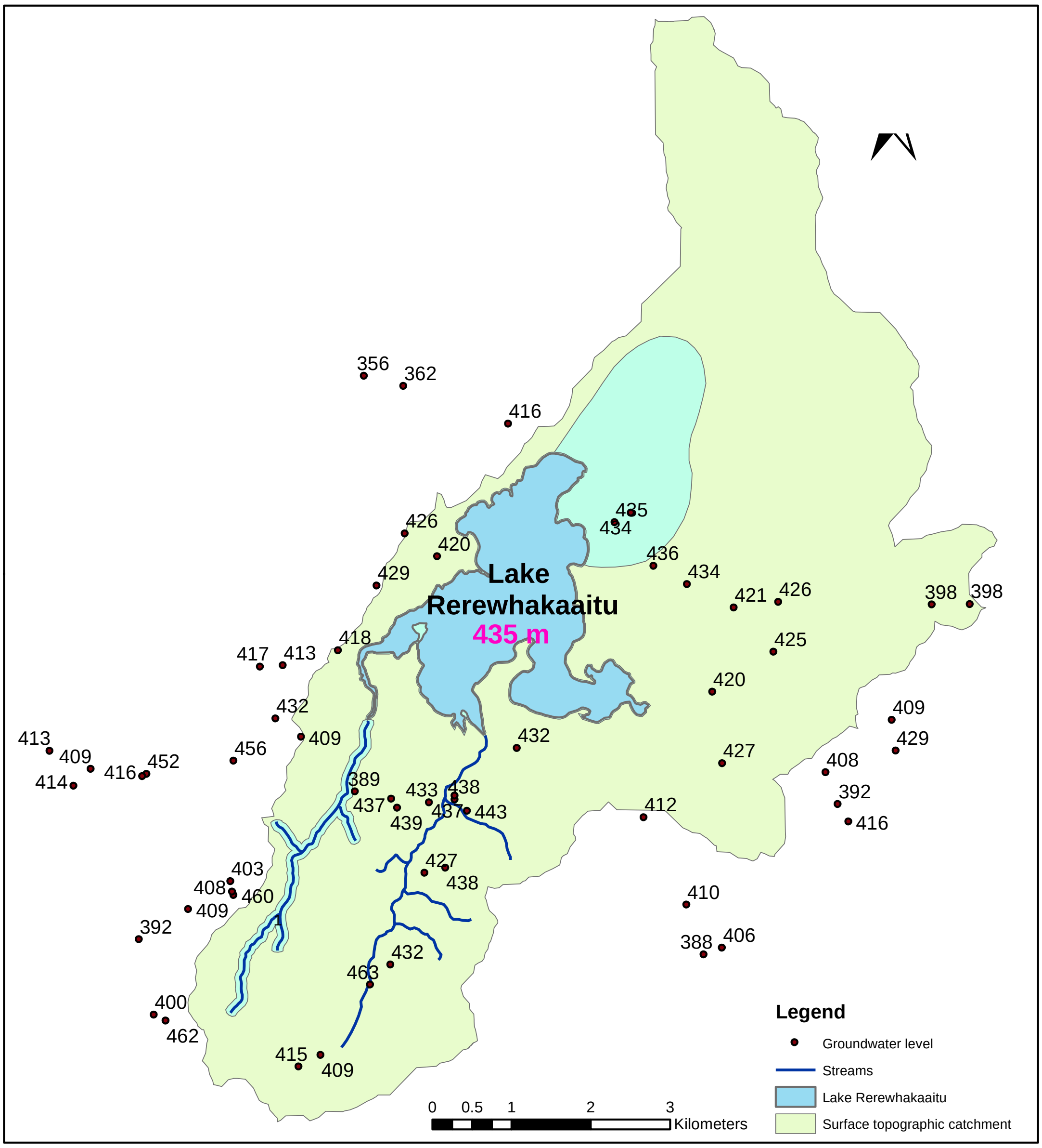

Figure 11. Elevation of groundwater (meters above mean sea level) in wells within and outside of the Lake Rerewhakaaitu topographic catchment (White et al. 2003). Colours denote topographic catchment, streams, lake and hydrological catchment (see caption).

Calibration and validation of DYRESM-CAEDYM

Water temperature and DO were calibrated using high frequency water column profiles, as shown in Fig. 12 (a)-(b) from July 2015 to May 2016. Parameter values were assigned within the range found in the literature except the critical wind speed and effective surface area coefficient, which were adjusted for best fit to data. The range of temperature and DO for surface and bottom waters and the maximum daily water column temperature and DO difference between surface and bottom waters are shown in Table 6. Bottom-water DO was highly variable depending on whether the water column was mixed or stratified, with mixing occurring along continuously after March.

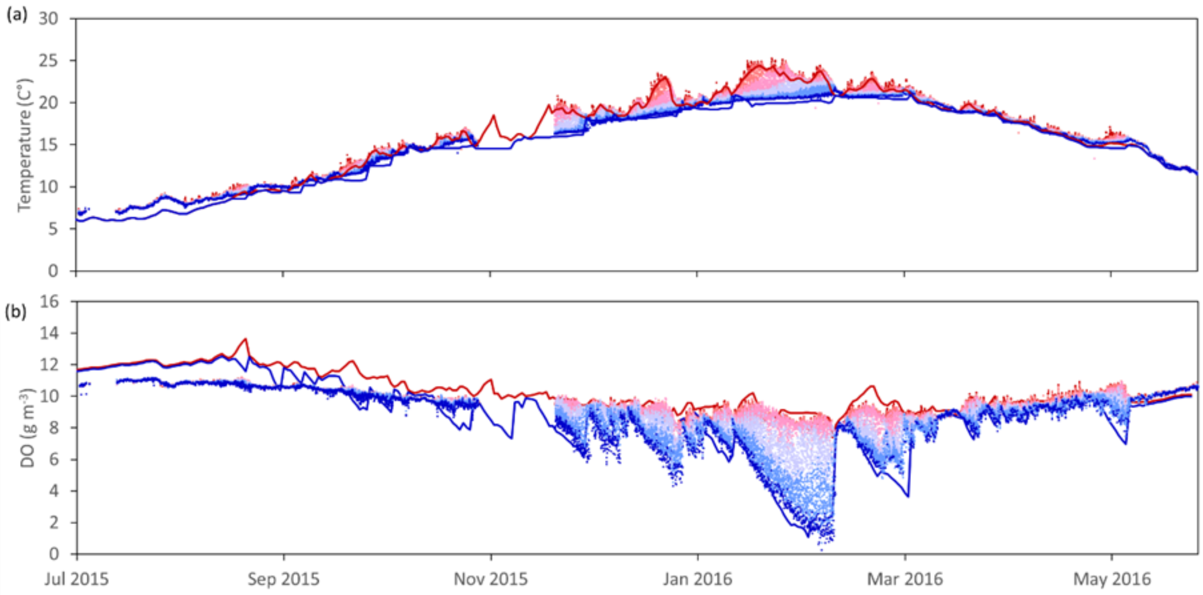

Figure 12. Model simulations (red and blue lines) and high frequency data (dots) for surface and bottom of the lake, for (a) water temperature, and (b) dissolved oxygen (DO) concentration for the calibration period of July 2015-May 2016. Red colour and blue colour indicate surface and bottom data, respectively.

Table 6. Temperature and dissolved oxygen (DO) ranges for surface (daily maximum) and bottom (daily minimum) water and maximum daily water column temperature and DO differences between surface and bottom from Jul 2015 to May 2016.

	Temperature	DO
Surface (1 m)	7.1 - 25.3 °C	8.1 - 11.2 g m^{-3}
Bottom (12 m)	6.7 - 21.2 °C	0.3 - 11.0 g m^{-3}
Max. difference	4.9 °C (surface: 25.3 °C, bottom: 20.4 °C)	8.7 g m^{-3} (surface: 9.0 g m^{-3}, bottom: 0.3 g m^{-3})

Temperature and DO were validated using monthly data for the period September 1992 to May 2016, as shown in Fig. 13 (a)-(d). Statistical comparison between model simulations and observed data (RMSE and NRMSE) were made at the surface (1 m), middle (6 m), and bottom (12 m) of the lake, as shown in Table 7. The model simulations indicated that stratification events occurred intermittently in summer, lasting for up to several days. These stratification events were most easily distinguished by a relatively linear decline in bottom DO, as shown in Fig. 12.

The model was calibrated from September 2013 to May 2016 for nutrients, SS, and total chlorophyll-*a* concentrations at the surface (1 m) and bottom (12 m), as well as Secchi depth, and also validated over 24-year period, using monthly data collected by BOPRC, as shown in Fig. 14-15. All parameters for sediment, nutrients, and phytoplankton were adjusted for best fit to observed data. Satisfactorily small values of RMSE and NRMSE indicated that model simulations generally approximated observed values accurately for both calibration and simulation periods (Table 7). Modelled and observed nutrient data at 6 m is shown in Fig 16. The calibrated values of parameters for sediments, nutrients, and phytoplankton for Lake Rerewhakaaitu are given in Tables 8 and 9.

Table 7. Statistical comparison of model simulation with field data for depths of 1 m, 6 m, and 12 m, using root mean squared error (RMSE) and normalized RMSE (NRMSE), for temperature (Temp.), concentrations of dissolved oxygen (DO), total nitrogen (TN), ammonium-N (NH_4-N), nitrate-N (NO_3-N), total phosphorus (TP), phosphate-P (PO_4-P), suspended solids (SS), and total chlorophyll-*a* (TChl-*a*), and Secchi depth.

	RMSE			NRMSE (%)		
	1 m	6 m	12 m	1 m	6 m	12 m
Temp. (C°)	0.7639	-	0.8103	4.5	-	5.9
DO (g m^{-3})	1.5602	-	1.7942	18.0	-	14.6
TN (g m^{-3})	0.0955	0.0928	0.0986	16.7	16.2	17.2
NH_4-N (g m^{-3})	0.0163	0.0169	0.0284	18.2	18.9	31.8
NO_3-N (g m^{-3})	0.0124	0.0135	0.0270	20.8	22.7	45.4
TP (g m^{-3})	0.0038	0.0037	0.0036	19.1	18.3	17.8
PO_4-P (g m^{-3})	0.0041	0.0043	0.0037	11.2	11.9	10.1
SS (g m^{-3})	0.5735	0.6556	0.7840	13.0	14.9	10.7
TChl-*a* (mg m^{-3})	2.58	-	-	13.7	-	-
Secchi depth (m)	2.47	-	-	25.8	-	-

Table 8. Parameters used in DYRESM for Lake Rerewhakaaitu

Parameter	Unit	Calibrated value	Reference
Critical wind speed	m s^{-1}	4.0	Best fit to data
Emissivity of water surface	-	0.96	Imberger & Patterson (1981)
Mean albedo of water	-	0.08	Patten et al. (1975)
Potential energy mixing efficiency	-	0.2	Spigel et al. (1986)
Shear production efficiency	-	0.08	Yeates and Imberger (2003)
Wind stirring efficiency	-	0.4	Spigel et al. (1986)
Vertical mixing coefficient	-	200	Yeates and Imberger (2003)
Effective surface area coefficient	m^2	1.5×10^7	Best fit to data

Table 9. Parameters used in CAEDYM for Lake Rerewhakaaitu

Parameter	Unit	Calibrated value
Sediment parameters		
Sediment oxygen demand	g m^{-2} d^{-1}	0.7
Half-saturation coefficient for sediment oxygen demand	g m^{-3}	1.0
Maximum potential PO_4-P release rate	g m^{-2} d^{-1}	0.0028
Oxygen half-saturation constant for release of PO_4-P from bottom sediments	g m^{-3}	1.5
Maximum potential NH_4-N release rate	g m^{-2} d^{-1}	0.013
Oxygen half-saturation constant for release of NH_4-N from bottom sediments	g m^{-3}	0.1
Maximum potential NO_3-N release rate	g m^{-2} d^{-1}	-0.03
Oxygen half-saturation constant for release of NO_3-N from bottom sediments	g m^{-3}	1.5
Temperature multiplier for nutrient release	-	1.06
Nutrient parameters		
Decomposition rate of POPL to DOPL	d^{-1}	0.017
Mineralisation rate of DOPL to PO_4-P	d^{-1}	0.07
Decomposition rate of PONL to DONL	d^{-1}	0.017
Mineralisation rate of DONL to NH_4-N	d^{-1}	0.016
Denitrification rate coefficient	d^{-1}	0.9
Oxygen half-saturation constant for denitrification	mg L^{-1}	1.5
Temperature multiplier for denitrification	-	1.03
Nitrification rate coefficient	d^{-1}	0.2
Nitrification half-saturation constant for oxygen	mg L^{-1}	1.5
Temperature multiplier for nitrification	-	1.03
Phytoplankton parameters		Cyanobacteria, Chlorophytes, Diatoms
Maximum potential growth rate at 20°C	d^{-1}	0.5, 1, 2.4
Irradiance parameter non-photoinhibited growth	µmol m^{-2} s^{-1}	300, 100, 15
Half saturation constant for phosphorus uptake	g m^{-3}	0.005, 0.003, 0.006
Half saturation constant for nitrogen uptake	g m^{-3}	0.04, 0.02, 0.06
Minimum internal nitrogen concentration	mg N (mg chl a)$^{-1}$	3, 4, 5
Maximum internal nitrogen concentration	mg N (mg chl a)$^{-1}$	11, 14, 12
Maximum rate of nitrogen uptake	mg N (mg chl a)$^{-1}$ d^{-1}	4.4, 8.8, 21.12
Minimum internal phosphorus concentration	mg P (mg chl a)$^{-1}$	0.4, 0.3, 0.2
Maximum internal phosphorus concentration	mg P (mg chl a)$^{-1}$	1.3, 2.5, 2
Maximum rate of phosphorus uptake	mg P (mg chl a)$^{-1}$ d^{-1}	0.63, 1.26, 3.024
Temperature multiplier for growth limitation	-	1.09, 1.10, 1.07
Standard temperature for growth	°C	20, 18, 14
Optimum temperature for growth	°C	32, 28, 23
Maximum temperature for growth	°C	39, 37, 30
Respiration rate coefficient	d^{-1}	0.05, 0.1, 0.24
Temperature multiplier for respiration	-	1.07, 1.06, 1.06
Fraction of respiration relative to total metabolic loss rate	-	0.8, 0.8, 0.8
Fraction of metabolic loss rate that goes to DOM	-	0.7, 0.7, 0.7
Constant settling velocity	m s^{-1}	5×10^{-7}, 0, -3×10^{-6}

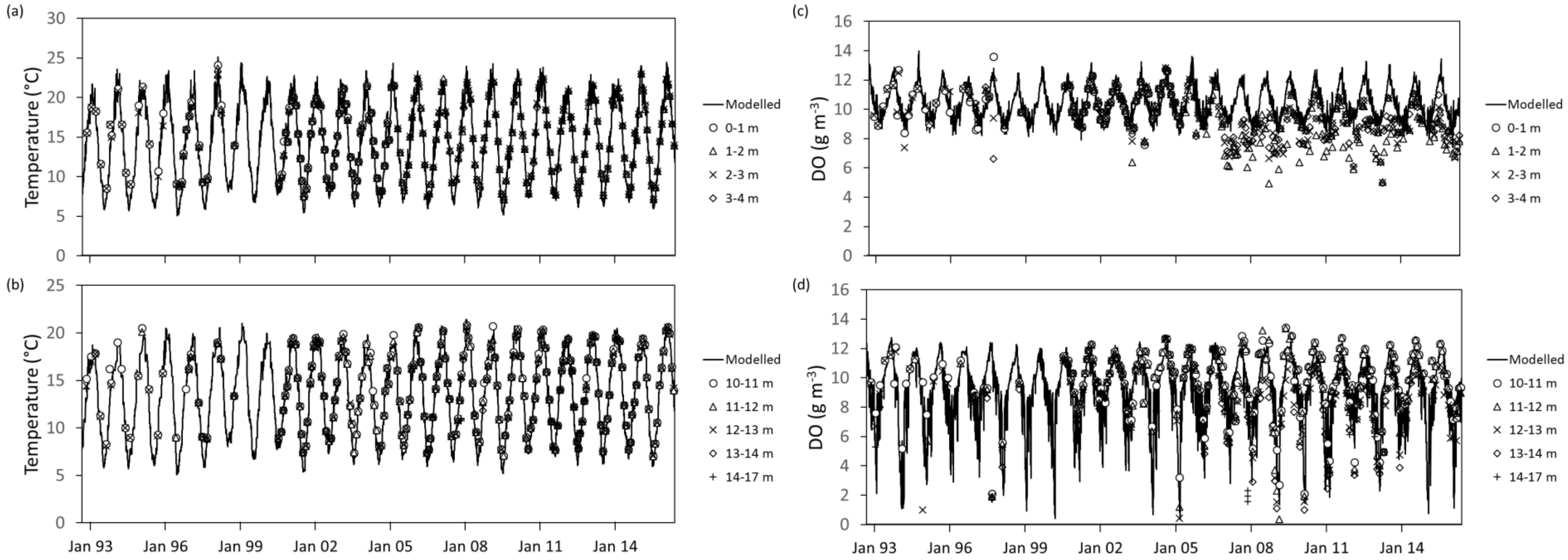

Figure 13. Model simulations (line) and observed data (dots) from BOPRC, for (a) water temperature on surface of the lake, (b) water temperature on bottom of the lake, (c) dissolved oxygen (DO) concentration on surface of the lake, and (d) dissolved oxygen concentration on bottom of the lake for the validation period of September 1992-May 2016.

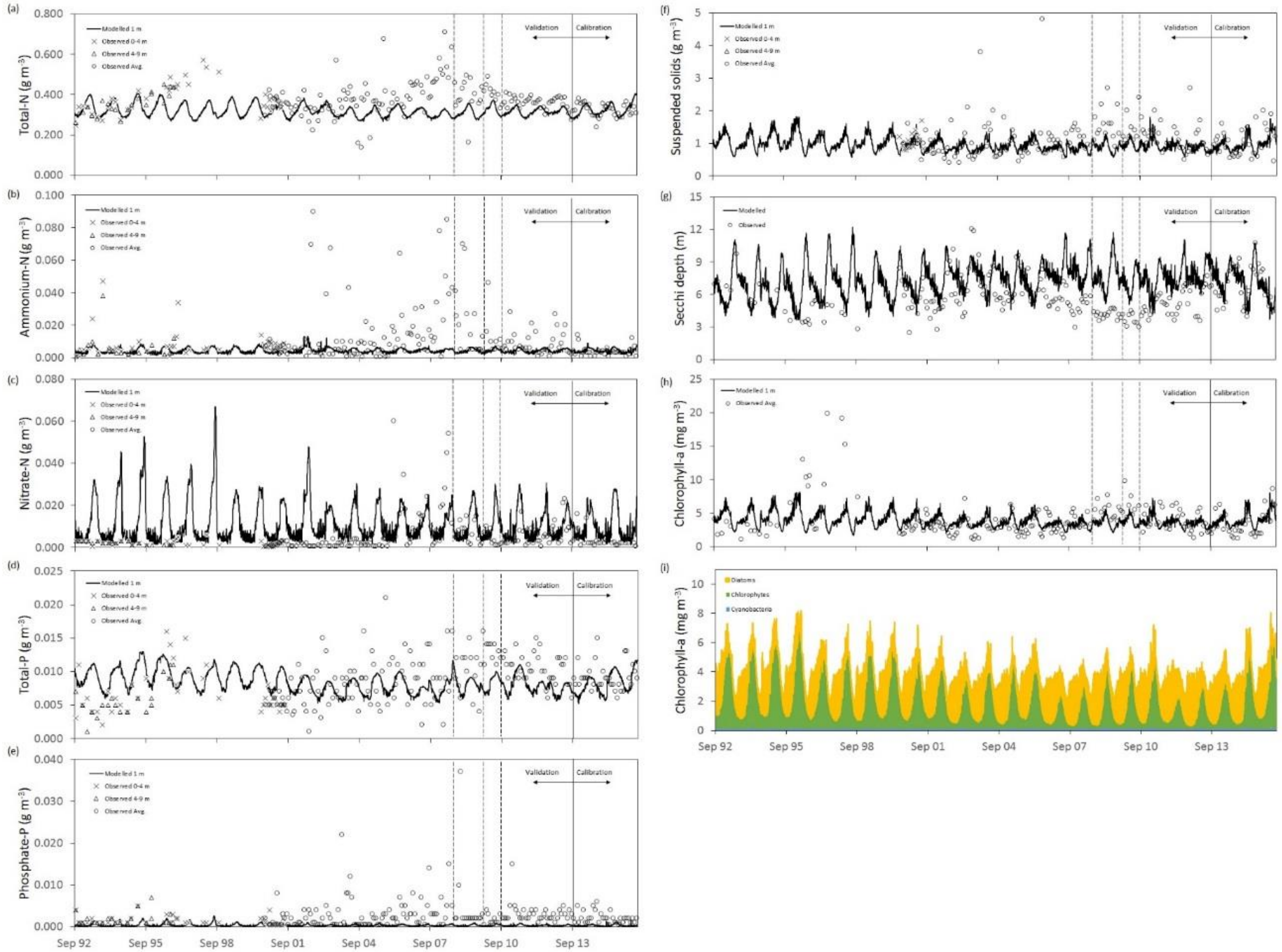

Figure 14. Model simulations for 1 m depth (line) and observed data (dots) for concentrations of (a) total nitrogen, (b) ammonium-N, (c) nitrate-N, (d) total phosphorus, (e) phosphate-P, and (f) suspended solids, (g) Secchi depth, (h) concentrations of total chlorophyll-*a*, and (i) the phytoplankton groups making up in total chlorophyll-*a*.

Symbols for (a)-(f) represent sample depth of observations. Modelled data in graph (a)-(f) and (h)-(i) was obtained at 1 m depth. Model calibration and validation periods are shown. Vertical long-dashed line shows lab changes from left to right: BOPRC (original), Hill, NIWA, and BOPRC (new) (see Methods).

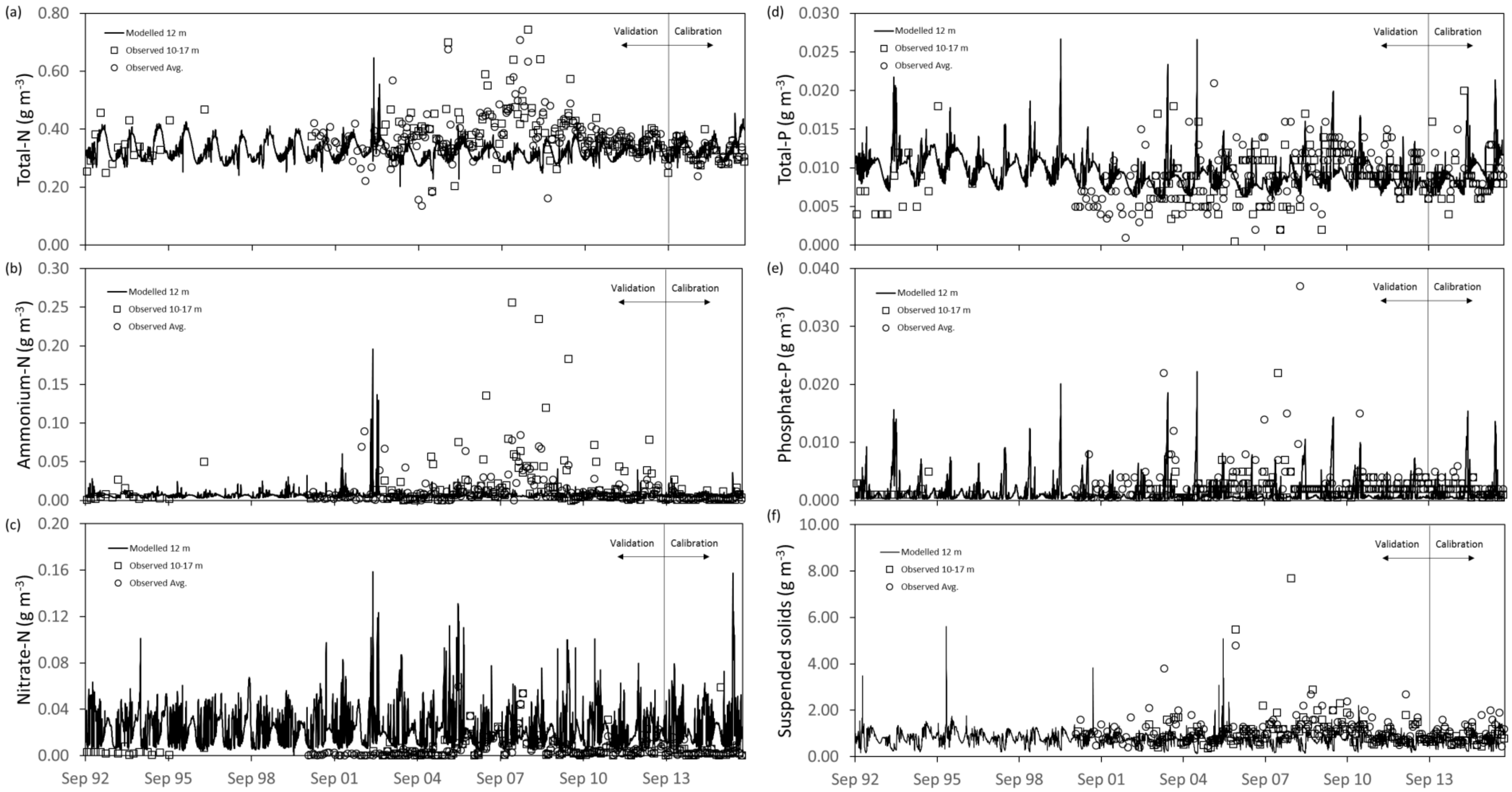

Figure 15. Model simulations for 12 m depth (line) and observed data (dots), for (a) total nitrogen, (b) ammonium-N, (c) nitrate-N, (d) total phosphorus, (e) phosphate-P, and (f) suspended solids concentrations in Lake Rerewhakaaitu. Rectangular dots and circles show observed data at 10-17 m depth and averages for the lake, respectively. The modelled data in the graph was obtained at 12 m depth in the lake. The calibration and validation periods are shown in the graphs.

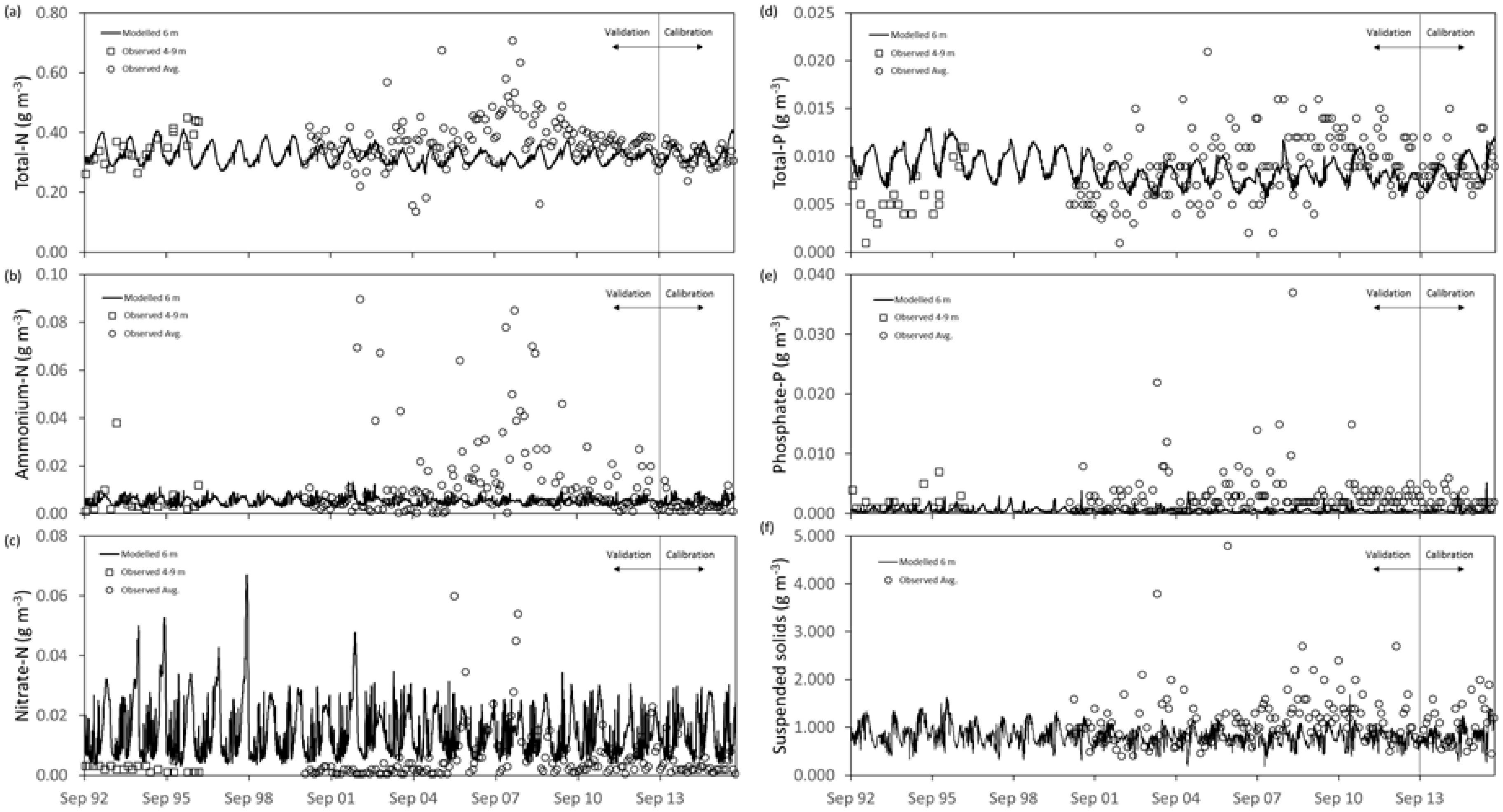

Figure 16. Comparison of model simulations 6 m depth (line) with observed data (dots), for (a) total nitrogen, (b) ammonium-N, (c) nitrate-N, (d) total phosphorus, (e) phosphate-P, and (f) suspended solids concentration. Rectangles and circles show observed data at 4-9 m depth and average of the lake, respectively. The modelled data in the graph is output at 6 m depth of the lake. The calibration and validation periods are shown in the graphs.

Effective forcing factor

The errors between observed and simulated data in 2006-2010 were large for DO, nutrients, and Secchi depth. We hypothesized that the error was related to daily change of forcing factors which were not included in the model input, because the model error was substantially greater during the mid-2000s. Therefore, one-to-one correspondence of daily error and daily forcing factors such as daily lake water level and daily meteorological data were plotted and analysed using linear regression.

Daily variations of lake water level, shortwave radiation, air temperature, and vapour pressure had a statistically significant linear relationship with the error of some model variables at the surface (1 m). Of these variables, lake water level was most closely related to errors in DO, total nitrogen, nitrate-N, total phosphorus, and Secchi depth (Fig. 17a-e). Shortwave radiation was significantly related to the errors in total nitrogen, nitrate-N, and total phosphorus. Air and wet bulb temperatures, and vapour pressure significantly affected errors in nitrate-N and total phosphorus. Linear regression models related to comparison of model error and different forcing variables are shown for all depths (1 m, 6 m and 12 m) in Tables 10 and 11.

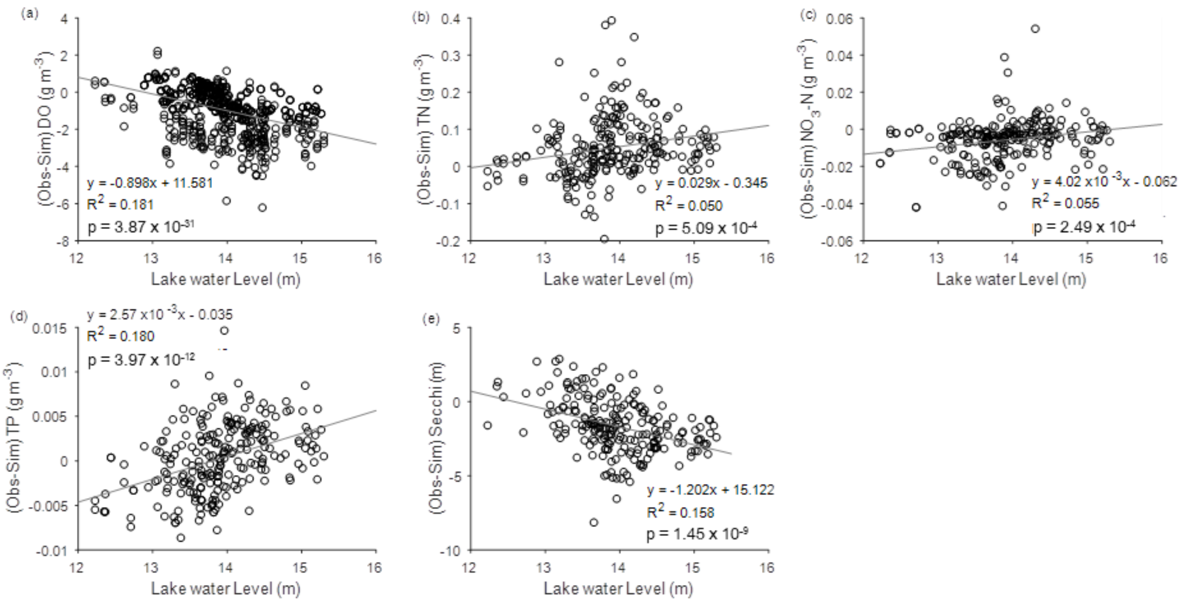

Figure 17. Linear regression model at the surface (1 m) for the error (Obs-Sim) of concentrations of (a) dissolved oxygen (DO), (b) total nitrogen (TN), (c) nitrate-N (NO_3-N), (d) and total phosphorus (TP), and (e) Secchi depth with lake water level for 1992-2016.

Table 10. Slope, y-intercept, p-value, and fraction of variation explained (R^2) by linear regression of lake water level and shortwave radiation intensity for the error (Obs-Sim) of concentrations of dissolved oxygen, total nitrogen (TN), ammonium-N (NH_4-N), nitrate-N (NO_3-N), total phosphorus (TP), phosphate-P (PO_4-P), suspended sediment (SS), and total chlorophyll-*a* (TChl-*a*), and Secchi depth. Bold indicates p-value < 0.05 (95 % confidence) and blue colour indicates p-value < 0.005 (99.5 % confidence).

	Lake water level				Short wavelength intensity			
	Slope	Y-intercept	p-value	R^2	Slope	Y-intercept	p-value	R^2
DO (1 m)	-0.898	11.581	**3.87 x10^{-31}**	0.181	-8.79 x10^{-5}	-0.950	0.876	3.64 x10^{-5}
DO (12 m)	-0.972	13.215	**5.87 x10^{-20}**	0.108	1.30 x10^{-3}	-0.711	0.081	4.16 x10^{-3}
TN (1 m)	0.028	-0.345	**5.09 x10^{-4}**	0.050	1.85 x10^{-4}	0.018	**2.02 x10^{-3}**	0.040
TN (6 m)	0.025	-0.300	**6.25 x10^{-3}**	0.037	1.57 x10^{-4}	0.019	**0.017**	0.028
TN (12 m)	0.019	-0.221	**0.011**	0.019	1.68 x10^{-4}	0.019	**1.98 x10^{-3}**	0.027
NH_4-N (1 m)	2.39 x10^{-3}	-0.027	0.113	0.010	1.91 x10^{-5}	3.13 x10^{-3}	0.078	0.013
NH_4-N (6 m)	2.42 x10^{-3}	-0.028	0.172	9.06 x10^{-3}	1.41 x10^{-5}	3.65 x10^{-3}	0.267	6.00 x10^{-3}
NH_4-N (12 m)	3.66 x10^{-3}	-0.043	0.122	6.72 x10^{-3}	4.27 x10^{-5}	1.43 x10^{-3}	**0.011**	0.018
NO_3-N (1 m)	4.02 x10^{-3}	-0.062	**2.49 x10^{-4}**	0.055	5.16 x10^{-5}	-0.015	**2.12 x10^{-11}**	0.173
NO_3-N (6 m)	4.74 x10^{-3}	-0.075	**4.10 x10^{-5}**	0.082	2.70 x10^{-5}	-0.013	**1.30 x10^{-3}**	0.051
NO_3-N (12 m)	6.52 x10^{-3}	-0.110	**1.63 x10^{-4}**	0.041	-4.56 x10^{-5}	-0.010	**2.40 x10^{-4}**	0.039
TP (1 m)	2.57 x10^{-3}	-0.035	**3.97 x10^{-12}**	0.180	1.05 x10^{-5}	-1.60 x10^{-3}	**1.36 x10^{-4}**	0.058
TP (6 m)	2.32 x10^{-3}	-0.032	**3.93 x10^{-9}**	0.157	8.66 x10^{-6}	-1.06 x10^{-3}	**2.84 x10^{-3}**	0.043
TP (12 m)	1.47 x10^{-3}	-0.021	**1.88 x10^{-6}**	0.063	4.33 x10^{-6}	-7.53 x10^{-4}	0.051	0.011
PO_4-P (1 m)	5.84 x10^{-4}	-5.85 x10^{-3}	0.092	0.012	1.51 x10^{-6}	2.00 x10^{-3}	0.545	1.50 x10^{-3}
PO_4-P (6 m)	5.15 x10^{-4}	-4.81 x10^{-3}	0.209	7.70 x10^{-3}	1.23 x10^{-6}	2.18 x10^{-3}	0.675	8.60 x10^{-4}
PO_4-P (12 m)	7.30 x10^{-4}	-8.89 x10^{-3}	**0.015**	0.016	-4.77 x10^{-6}	2.19 x10^{-3}	**0.025**	0.014
SS (1 m)	0.080	-0.931	0.266	6.35 x10^{-3}	3.02 x10^{-4}	0.140	0.513	2.20 x10^{-3}
SS (6 m)	0.049	-0.367	0.519	2.29 x10^{-3}	1.07 x10^{-3}	0.143	**0.031**	0.025
SS (12 m)	0.016	0.120	0.811	1.68 x10^{-4}	8.82 x10^{-4}	0.196	0.050	0.011
TChl-*a*	0.547	-7.574	0.062	0.016	-3.90 x10^{-3}	0.748	0.056	0.017
Secchi depth	-1.202	15.122	**1.45 x10^{-9}**	0.158	1.80 x10^{-3}	-1.992	0.207	7.45 x10^{-3}

Table 11. Slope, y-intercept, p-value, and fraction of variation explained (R2) for linear regression of air temperature, vapour pressure, and wet temperature on the error (Obs-Sim) of concentrations dissolved oxygen DO), total nitrogen (TN), ammonium-N (NH_4-N), nitrate-N (NO_3-N), total phosphorus (TP), phosphate-P (PO_4-P), suspended sediment (SS), and total chlorophyll-*a* (TChl-*a*), and Secchi depth. Bold indicates p-value < 0.05 (95 % confidence) and blue colour indicates p-value < 0.005 (99.5 % confidence).

	Air temperature				Vapour pressure				Wet temperature			
	Slope	Y-intercept	p-value	R^2	Slope	Y-intercept	p-value	R^2	Slope	Y-intercept	p-value	R^2
DO (1 m)	-6.21 x10^{-3}	-0.889	0.596	4.17 x10^{-4}	-0.021	-0.711	0.163	2.88 x10^{-3}	-0.019	-0.615	0.165	3.43 x10^{-3}
DO (12 m)	0.065	-1.289	**4.22 x10^{-5}**	0.023	0.066	-1.291	**1.39 x10^{-3}**	0.014	0.066	-1.063	**6.50 x10^{-4}**	0.019
TN (1 m)	2.86 x10^{-3}	0.015	**0.030**	0.020	4.24 x10^{-3}	-6.41 x10^{-4}	**0.014**	0.025	3.70 x10^{-3}	0.021	**0.023**	0.027
TN (6 m)	2.01 x10^{-3}	0.022	0.160	0.010	2.71 x10^{-3}	0.014	0.148	0.011	2.63 x10^{-3}	0.031	0.147	0.013
TN (12 m)	2.12 x10^{-3}	0.022	0.061	0.010	2.88 x10^{-3}	0.014	0.052	0.011	2.86 x10^{-3}	0.035	**0.048**	0.015
NH_4-N (1 m)	5.44 x10^{-4}	-2.28 x10^{-4}	**0.019**	0.022	7.76 x10^{-4}	-2.88 x10^{-3}	**0.011**	0.026	6.34 x10^{-4}	1.04 x10^{-3}	**0.030**	0.023
NH_4-N (6 m)	4.03 x10^{-4}	1.11 x10^{-3}	0.137	0.011	6.34 x10^{-4}	-1.60 x10^{-3}	0.072	0.016	5.23 x10^{-4}	2.13 x10^{-3}	0.135	0.014
NH_4-N (12 m)	1.38 x10^{-3}	-8.34 x10^{-3}	**6.59 x10^{-5}**	0.044	1.88 x10^{-3}	-0.014	**3.01 x10^{-5}**	0.048	1.78 x10^{-3}	-7.56 x10^{-3}	**1.24 x10^{-4}**	0.053
NO_3-N (1 m)	1.27 x10^{-3}	-0.022	**3.96 x10^{-14}**	0.216	1.47 x10^{-3}	-0.024	**2.87 x10^{-11}**	0.171	1.27 x10^{-3}	-0.019	**1.49 x10^{-9}**	0.171
NO_3-N (6 m)	4.73 x10^{-4}	-0.014	**0.010**	0.033	4.88 x10^{-4}	-0.015	**0.042**	0.021	4.05 x10^{-4}	-0.013	0.086	0.019
NO_3-N (12 m)	-1.72 x10^{-3}	3.16 x10^{-3}	**2.05 x10^{-11}**	0.123	-2.21 x10^{-3}	8.62 x10^{-3}	**3.30 x10^{-11}**	0.120	-1.84 x10^{-3}	8.92 x10^{-4}	**2.91 x10^{-8}**	0.111
TP (1 m)	2.83 x10^{-4}	-3.24 x10^{-3}	**1.44 x10^{-6}**	0.091	3.91 x10^{-4}	-4.46 x10^{-3}	**3.70 x10^{-7}**	0.101	3.26 x10^{-4}	-3.34 x10^{-3}	**4.93 x10^{-6}**	0.098
TP (6 m)	2.05 x10^{-4}	-2.08 x10^{-3}	**9.27 x10^{-4}**	0.052	2.80 x10^{-4}	-2.94 x10^{-3}	**5.41 x10^{-4}**	0.057	2.33 x10^{-4}	-2.12 x10^{-3}	**2.62 x10^{-3}**	0.054
TP (12 m)	4.35 x10^{-5}	-5.41 x10^{-4}	0.346	2.53 x10^{-3}	8.07 x10^{-5}	-9.82 x10^{-4}	0.180	5.12 x10^{-3}	4.69 x10^{-5}	-5.40 x10^{-4}	0.414	2.48 x10^{-3}
PO_4-P (1 m)	5.15 x10^{-5}	1.63 x10^{-3}	0.338	3.76 x10^{-3}	6.69 x10^{-5}	1.46 x10^{-3}	0.342	3.70 x10^{-3}	6.20 x10^{-5}	1.67 x10^{-3}	0.362	4.10 x10^{-3}
PO_4-P (6 m)	3.24 x10^{-5}	1.99 x10^{-3}	0.605	1.31 x10^{-3}	4.23 x10^{-5}	1.88 x10^{-3}	0.605	1.31 x10^{-3}	4.42 x10^{-5}	2.04 x10^{-3}	0.590	1.77 x10^{-3}
PO_4-P (12 m)	-1.41 x10^{-4}	3.11 x10^{-3}	**1.47 x10^{-3}**	0.028	-1.68 x10^{-4}	3.41 x10^{-3}	**3.56 x10^{-3}**	0.024	-1.34 x10^{-4}	2.85 x10^{-3}	**0.023**	0.019
SS (1 m)	-0.013	0.357	0.150	0.011	-0.018	0.407	0.140	0.011	-0.020	0.430	0.082	0.020
SS (6 m)	0.012	0.177	0.243	7.48 x10^{-3}	0.014	0.159	0.301	5.87 x10^{-3}	4.89 x10^{-3}	0.306	0.709	9.92 x10^{-4}
SS (12 m)	0.010	0.221	0.273	3.54 x10^{-3}	0.013	0.190	0.284	3.38 x10^{-3}	3.31 x10^{-3}	0.372	0.788	2.83 x10^{-4}
TChl-a	-0.061	0.825	0.165	9.11 x10^{-3}	-0.022	0.335	0.707	6.73 x10^{-4}	-0.053	0.765	0.343	5.29 x10^{-3}

Secchi	0.055	-2.355	0.069	0.015	0.035	-2.109	0.369	3.79×10^{-3}	0.057	-2.489	0.106	0.015

Scenario analysis

Simulation results for six scenarios differentiated by land use intensity, i.e., ‘Current‘, ‘Stream‘, and ‘High-production‘, and by climate, i.e., ‘Forest_CC‘, ‘Current_CC‘, and ‘High-production_Stream_CC‘, are shown as box plots for lake water level, temperature, and DO in Fig. 18, for nutrients and SS in Fig. 19, and for phytoplankton biomass and Secchi depth in Fig. 20. The percentage difference in these variables between the scenarios based on comparison with the ‘Current’ value are summarized in Table 12, with absolute median values summarized in Table 13.

The land use intensification scenarios involved an increase extrapolation of nutrient concentrations in streams (Stream) and/or intensified land use (High-production). The 'Stream' scenario followed the linear regression with logarithmic transformation model (see section 3.2), for increases of nitrate-N and phosphate-P concentrations in Mangakino and Awaroa streams. The 'High-production' scenario assumed that all of the effective hydrological catchment was high-production grassland. When the average concentrations in 2003-2012 and in 2090-2099 were compared, the average concentrations of total nitrogen and total phosphorus increased 1.4 times in Mangakino stream catchment, 1.7 times in Awaroa stream catchment, and 3.4-3.9 times in groundwater inflow catchment and runoff area, respectively.

'High-production' showed a greater increase in lake water nutrient concentrations than the 'Stream', and 'Stream' showed the greatest relative increase of nitrate-N amongst all nutrients. In both ’High-production’ and ‘Stream’, diatoms increased and chlorophytes decreased, with the magnitude of the change greater for the ‘High-production’ scenario than the ‘Stream’ scenario.

Scenarios of climate change included all forest with climate change (Forest_CC), current land use with climate change (Current_CC), and intensified land use and increased of nutrient concentrations in streams with climate change (High-production_Stream_CC). The median lake water level with climate change decreased 0.7 m. The median water temperature at the surface and bottom in the lake increased. Additionally, climate change resulted in increased total nitrogen, total phosphorus, SS and total chlorophyll-*a* concentrations, and decreased Secchi depth. Relative biomass of phytoplankton shifted away from diatoms and towards chlorophytes, principally due to substantial increase in chlorophyte biomass.

As land use was intensified from 'Forest_CC' to 'Current_CC' and 'High-production_Stream_CC' within the climate change scenarios, nutrients concentrations and total chlorophyll-*a* increased and Secchi depth decreased. Among climate change scenarios, 'Forest_CC' had the greatest decrease in diatoms and increase in chlorophytes and cyanobacteria, while ‘High-production_Stream_CC’ had the smallest decrease in diatoms and smallest increase in chlorophytes, and cyanobacteria.

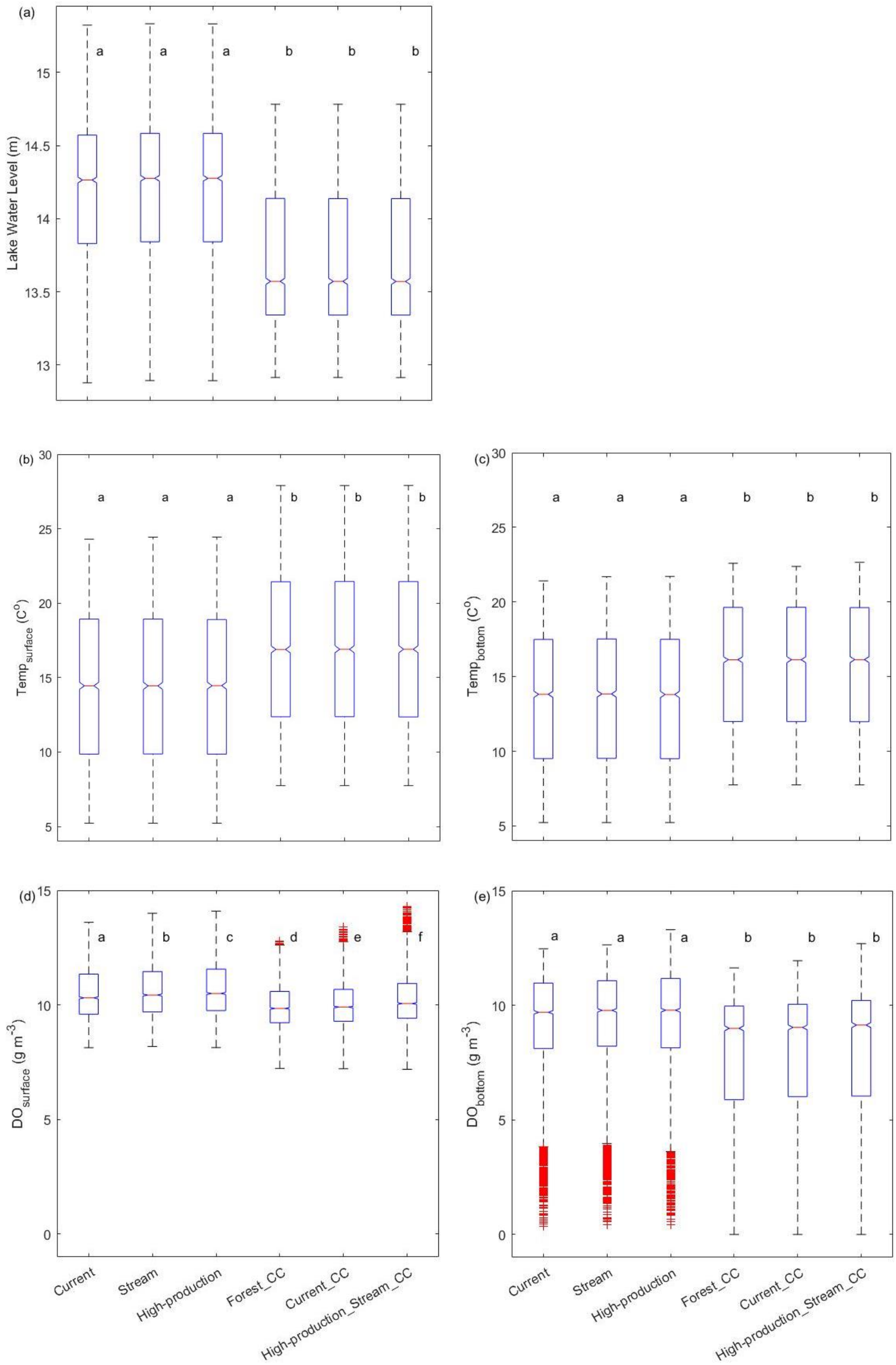

Figure 18. Box plots with One-Way ANOVA for model scenarios for a) lake water level, b) surface water temperature, c) bottom water temperature, d) surface dissolved oxygen concentration, and e) bottom dissolved oxygen concentration. Letters represent statistically similar values for each variable based on a Tukey's post-hoc test. Boxes represent 25th, 50th and 75th percentiles with red points denoting outliers.

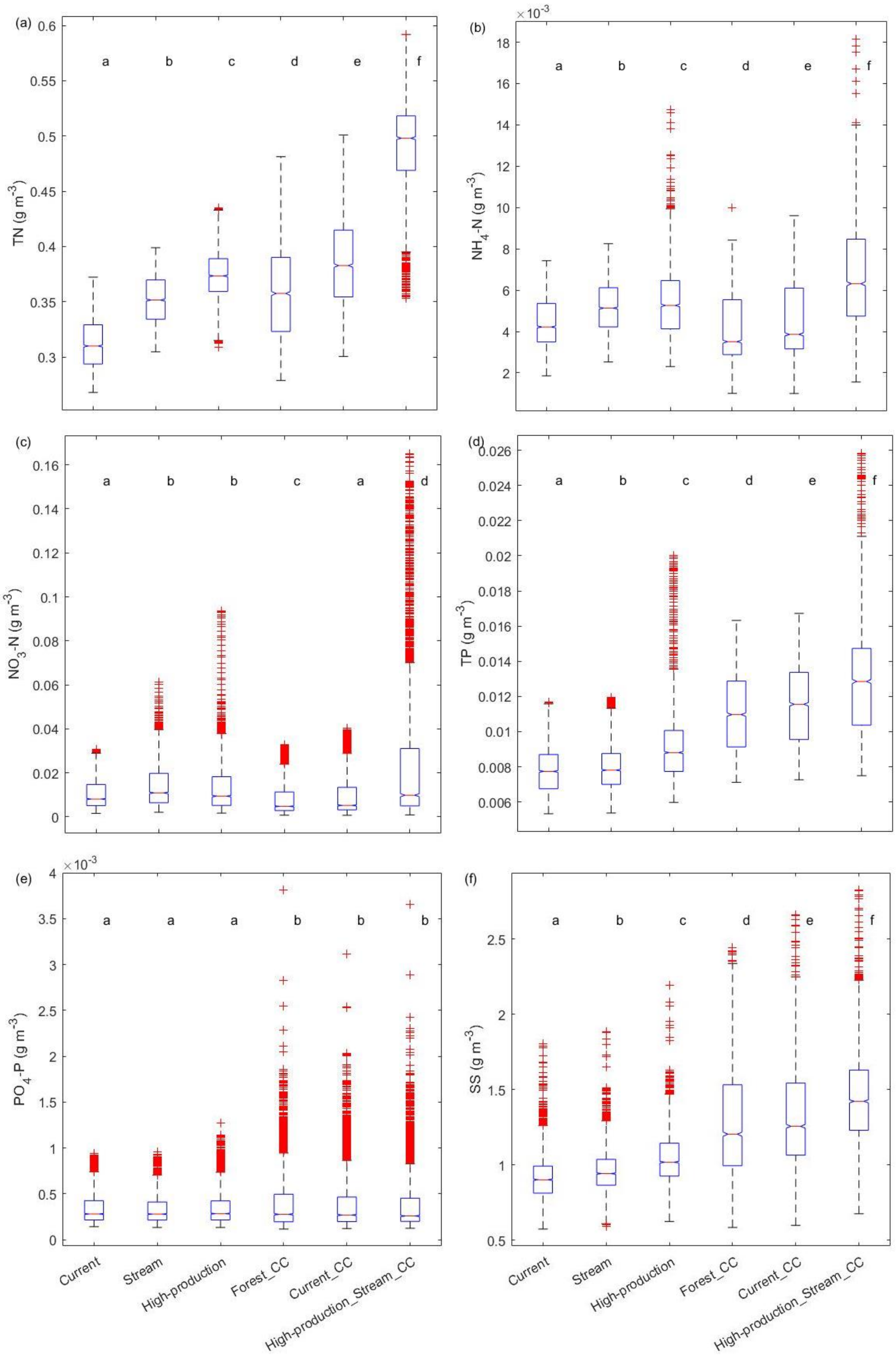

Figure 19. Box plots with One-Way ANOVA for model scenarios for a) total nitrogen (TN), b) ammonium-N (NH_4-N), c) nitrate-N (NO_3-N), d) total phosphorus (TP), e) phosphate-P (PO_4-P), (f) suspended solids (SS) concentration. A Tukey's post-hoc test revealed significance groups, represented by letters. Boxes represent 25th, 50th and 75th percentiles with red points denoting outliers.

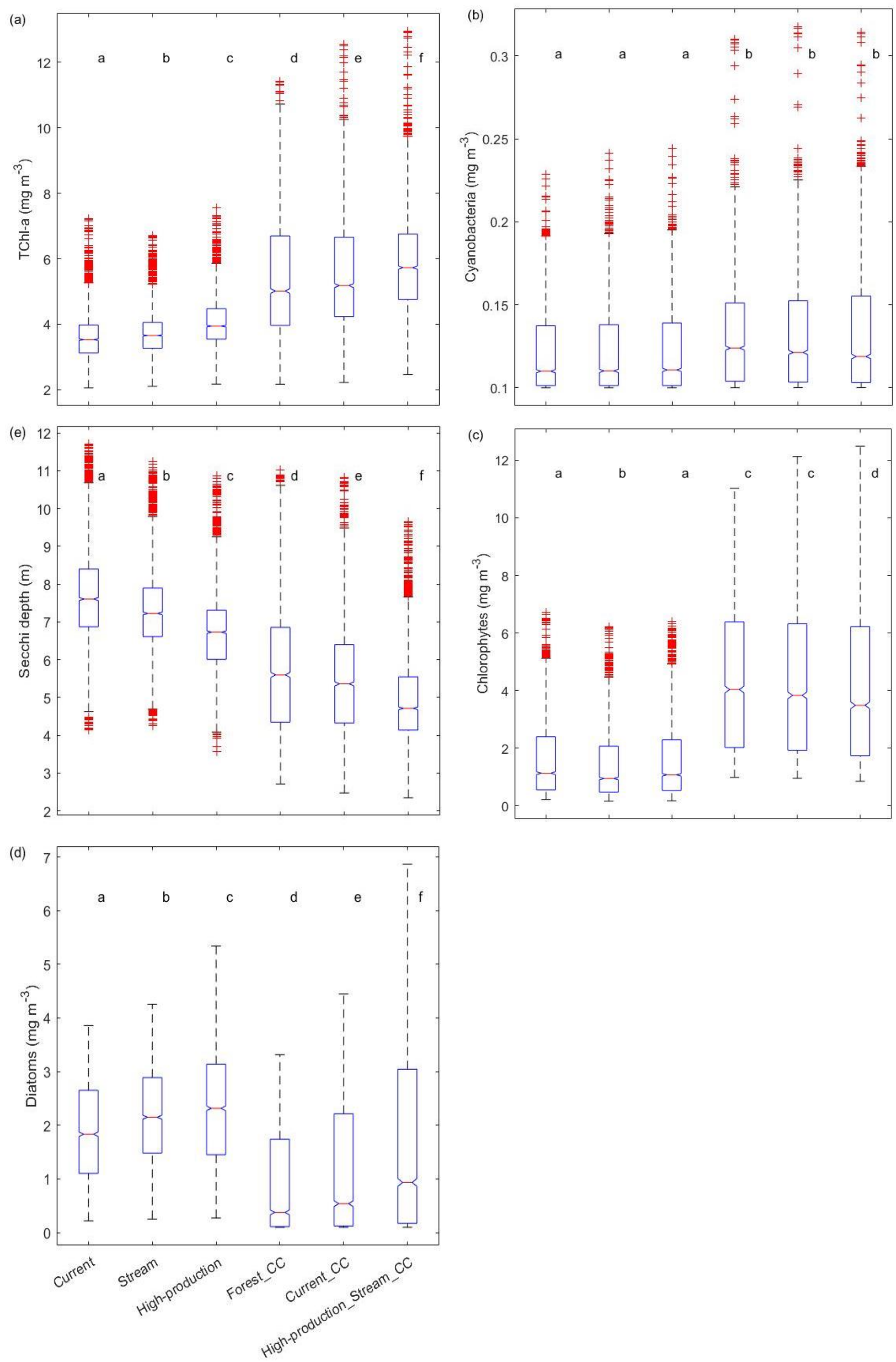

Figure 20. Box plots with One Way ANOVA for all scenario simulations, for a) total chlorophyll-*a* (TChl-*a*), b) cyanobacteria chlorophyll, c) chlorophyte chlorophyll, d) diatom chlorophyll, and e) Secchi depth. A Tukey's post-hoc test revealed significance groups, represented by letters. Boxes represent 25th, 50th and 75th percentiles with red points denoting outliers.

Table 12. Difference of median value by percentage between 'Current' and each scenario. Red and blue colours show the intensity of increase or decrease of each variable, respectively. Temperature (Temp), dissolved oxygen (DO), total nitrogen (TN), ammonium-N (NH_4-N), nitrate-N (NO_3-N), total phosphorus (TP), phosphate-P (PO_4-P), suspended sediment (SS), and total chlorophyll-*a* (TChl-*a*), and Secchi depth

	Land use intensification scenarios			Climate change scenarios		
	Current	Stream	High-production	Forest_CC	Current_CC	High-production _Stream_CC
Lake water level	0%	0%	0%	-5%	-5%	-5%
Temp (Surface)	0%	0%	0%	17%	17%	17%
Temp (Bottom)	0%	0%	0%	17%	17%	17%
DO (Surface)	0%	1%	2%	-4%	-4%	-2%
DO (Bottom)	0%	1%	1%	-7%	-7%	-6%
TN	0%	13%	20%	15%	23%	61%
NH_4-N	0%	22%	25%	-17%	-8%	50%
NO_3-N	0%	34%	16%	-41%	-36%	22%
TP	0%	1%	14%	42%	49%	66%
PO_4-P	0%	-1%	1%	-1%	-4%	-8%
SS	0%	5%	13%	34%	39%	58%
TChl-a	0%	4%	12%	42%	47%	62%
Cyanobacteria	0%	0%	1%	13%	10%	8%
Chlorophytes	0%	-16%	-5%	256%	238%	208%
Diatoms	0%	17%	26%	-79%	-71%	-49%
Secchi depth	0%	-5%	-12%	-26%	-29%	-38%

Table 13. Absolute lake median values for output from DYRESM-CAEDYM scenarios for changes in land use, stream concentrations and climate. Temperature (Temp), dissolved oxygen (DO), total nitrogen (TN), ammonium-N (NH_4-N), nitrate-N (NO_3-N), total phosphorus (TP), phosphate-P (PO_4-P), suspended sediment (SS), and total chlorophyll-*a* (TChl-*a*), and Secchi depth

	Land use intensification scenarios			Climate change scenarios		
	Current	Stream	High-production	Forest_CC	Current_CC	High-production _Stream_CC
Lake water level (m)	14.3	14.3	14.3	13.6	13.6	13.6
Temp (Surface) (C°)	14.5	14.4	14.5	16.9	16.9	16.9
Temp (Bottom) (C°)	13.8	13.8	13.8	16.1	16.1	16.1
DO (Surface) (g m^{-3})	10.3	10.4	10.5	9.8	9.9	10.1
DO (Bottom) (g m^{-3})	9.7	9.8	9.8	9.0	9.0	9.1
TN (g m^{-3})	0.31	0.35	0.37	0.36	0.38	0.50
NH_4-N (g m^{-3})	4.2×10^{-3}	5.1×10^{-3}	5.3×10^{-3}	3.5×10^{-3}	3.9×10^{-3}	6.3×10^{-3}
NO_3-N (g m^{-3})	8.1×10^{-3}	0.01	9.4×10^{-3}	4.8×10^{-3}	5.2×10^{-3}	9.9×10^{-3}
TP (g m^{-3})	7.7×10^{-3}	7.8×10^{-3}	8.8×10^{-3}	0.01	0.01	0.01
PO_4-P (g m^{-3})	2.8×10^{-4}	2.8×10^{-4}	2.8×10^{-4}	2.8×10^{-4}	2.7×10^{-4}	2.6×10^{-4}
SS (g m^{-3})	0.9	0.9	1.0	1.2	1.3	1.4
TChl-a (mg m^{-3})	3.5	3.7	3.9	5.0	5.2	5.7
Cyanobacteria (mg m^{-3})	0.11	0.11	0.11	0.12	0.12	0.12
Chlorophytes (mg m^{-3})	1.13	0.95	1.08	4.04	3.84	3.49
Diatoms (mg m^{-3})	1.83	2.15	2.32	0.38	0.54	0.93
Secchi depth (m)	7.6	7.2	6.7	5.6	5.4	4.7

Discussion

When the time trend of nutrient concentrations in the lake from 2000 was statistically analyzed using the Mann-Kendall test and linear regression model, total phosphorus and nitrate-N concentrations showed a linear increase. Nitrate concentrations in the Mangakino and Awaroa streams also increased significantly over the monitoring 20-year period (Mann-Kendall test and linear regression with logarithmic transformation model). These changes likely reflect the effect of land use intensification in the lake catchment, with some apparent lag. Most other nutrient species, some of which showed weak increasing trends in the streams, did not appear to have a corresponding impact on lake concentrations. This likely reflects the relatively small contribution to the lake water balance of surface stream discharge.

Hydraulic modelling was performed to determine inflows to and outflows from the lake. As evidenced by the relatively small model error in water level, the time series dynamics of groundwater inflow, surface runoff to the lake and precipitation, are relatively well balanced with losses to the surface outlet (which flows only occasionally) and groundwater losses, as well as evaporation. Rainfall is the main source of water to the lake relative to surface water inflows, and groundwater outflow is the main outflow from the lake, as noted by White et al. (2003). Groundwater outflow was more than twice as large as the groundwater inflow.

As a result of the lake water balance using coupled output from a groundwater model (MODFLOW) and a lake model (DYRESM-CAEDYM), the effective hydrological catchment (the 'water sensitive zone' of the surface topographic catchment) was identified to be only 10% of the surface catchment. McColl (1972) reported the relationship between silica content in lakes and their surface catchment area, finding that high silica concentrations occurred in lakes with large surface catchment area. Chapman et al. (1981) reported that the silica concentration of Lake Rerewhakaaitu was lower than was predicted from catchment area using the relationship established by McColl (1972), so he assumed that Lake Rerewhakaaitu was an exception. However, the relationship between silica content in the lake and surface catchment area is well matched when the area of the effective hydrological catchment, rather than the surface topographic catchment, is used. In addition, the effective hydrological catchment provides a better fit for the relation between the percentage of the catchment in pasture or urban land use and the Trophic Level Index (TLI) across all of the Rotorua lakes (Scholes and Hamill 2016). The difference between the topographic catchment and the effective hydrological catchment explains why water quality in this lake has not been substantially affected by intensive agricultural development.

From the water quality model results, the lake is generally well mixed, but with multiple stratification events occurring during summer (mostly December-February). Phosphate concentrations are low compared with other Rotorua Te Arawa lakes, likely because of absorption onto colloidal allophanic clays (Fish 1978), and possibly because of a high relative contribution of water by rainfall direct to the lake. Among nitrogen species, organic nitrogen was dominant (95% on average), compared with inorganic nitrogen forms of ammonium-N (4 %) and nitrate-N (1 %). Fish (1978) found no relationship between Secchi depth and total chlorophyll-*a*, but this may have been related to low chlorophyll-*a* concentrations as theoretically such a relationship is inherent. Diatoms and chlorophytes were modelled as the dominant species, with some seasonal variation (diatoms being greater in winter), and cyanobacteria rarely occurred. The lake is on balance mesotrophic according to TLI value (Burns et al. 2009, Scholes and Hamill 2016).

During the 24-year simulation, differences between observations and simulations were most noticeable for the period 2006-2010. During this period, simulated DO concentration and Secchi depth were lower than observations and observed nutrients were generally higher. Some of this error appears to be systematic (at least in terms of nutrients), likely related to discrete periods of change associated with changes in laboratories performing the analysis. Measurements were made by BOPRC until August 2008, at Hill Laboratories until December 2009, at NIWA until September 2010, and then again at BOPRC (Fig. 14). Analytical detection methods and detection limits varied amongst laboratories and there was an indication that variability in phosphate-P concentrations was greatly reduced for some labs. Overall, however, there was no relationship between the lab change and the error between observations and simulations.

We examined the effect of forcing factors which were not reflected in the model input and presented a novel uncertainty analysis that allows for assessment of forcing factors that contribute to model error. High values of lake water level tended to lead to greater model error. Possible reasons for this may relate to wind-driven resuspension of sediment with high nitrogen and phosphorus content when lake water levels are high (McIntosh et al. 2001, Reeves et al. 2008). It is also possible that macrophytes (which were not simulated in this study) might affect water quality. High lake water level could result in a reduction in submerged macrophyte bed extent due to poor light conditions and these conditions would also be associated with low Secchi disk depths (Pereira et al. 2012).

Errors in total nitrogen, nitrate-N, and total phosphorus were statistically significantly related to shortwave radiation intensity, dry and wet bulb air temperature, and vapour pressure, though with low levels of variation explained. It is unclear whether these relationships are meaningful.

For the scenario analysis, changes in land use intensity were relatively straightforward and related to increased nutrient loading and total chlorophyll-*a*. Effects from climate change were more complex as they affected multiple variables directly, including lake water level and water temperature, and indirectly via changes in stratification of temperature and DO, changes in nutrients and subsidiary effects on phytoplankton biomass and species composition.

Due to climate change, the lake water level decreased (see projections for climate change impacts by MacKay et al. 2009, Paerl and Huisman 2009). This change was associated with decreased precipitation and increased evaporation from the lake. High air and water temperatures, high shortwave radiation, and low humidity caused high evaporation rates. In scenarios of climate change, 10-year average precipitation decreased 6.6 L s^{-1} while evaporation increased 7.3 L s^{-1}. Average atmospheric temperature increased, so average inflow water temperature also increased by 2.2 °C based on changes in air temperature. In scenarios of climate change, the stratification of temperature and DO became stronger, noticeably with lower levels of DO in bottom waters. Averaged wind speed decreased while air temperature increased, leading to an increase in median water temperature in the lake by c. 2.4 °C, concurrent with increased stratification.

The major species of phytoplankton changed from diatoms to chlorophytes under the climate change scenarios. Interestingly, the land use intensification scenarios showed a slight increase in diatoms. The main reason for the differences between scenarios is likely to be increased water temperature which may be physiologically advantageous for chlorophytes (Hamilton et al. 2016) but the low-nutrient conditions in the lake did not lead to temperature-tolerant cyanobacteria as has been predicted in other climate change studies of lakes with higher trophic state (Paerl and Huisman 2009, Hamilton et al. 2016). This may be because Rerewhakaaitu currently does not sustain substantial populations of cyanobacteria with which to accurately parameterise their life cycle within the lake. Nutrient mineralization rates and releases from sediments are expected to increase with increasing water temperature (Jensen and Andersen 1992), as well as the lower levels of DO with climate change. Overall, the modelled effect of climate change on lake nutrients is likely to have a greater impact on lake water quality than that of land use intensification. Total chlorophyll-*a* increased 12% with a highly hypothetical scenario of all of the hydrological catchment converted to high-production grassland, while total chlorophyll-*a* increased 47% in the climate change scenarios in the absence of any change in land use. Runoff in winter is expected to be greater with climate change due to higher intensity rainfall events (Jeppesen et al. 2009; Hamilton et al. 2014), even though annual precipitation is likely to decrease.

The change of land use from high producing grassland, which accounts for 27% of the effective hydrological catchment, to planted forest could slightly offset the effect of climate change. This management strategy could provide some ability to reduce nutrient concentrations and total chlorophyll-*a* in the presence of climate warming, though it did not prevent increases in chlorophytes or cyanobacteria in the lake model simulations. Reducing losses of nutrients from the hydrologically effective catchment and enhancing vegetation in the riparian area around the lake represent viable options to combat declining water quality of Lake Rerewhakaaitu in the presence of climate change.

Conclusions

Long-term analysis of nutrient concentrations in Lake Rerewhakaaitu and stream inflows showed statistically significant increases of some nutrients (nitrate and total phosphorus), suggesting a need for vigilant catchment management. However, the unusual hydrological characteristics of Lake Rererewhakaaitu, with the effective hydrological catchment being approximately one-tenth of the topographic catchment, mean that catchment management initiatives not targeted at the hydrologically effective catchment, will have very limited impact on lake water quality. Scenario analyses involving various combinations of changes in land use intensity and climate change showed that climate change effects are likely to a have greater impact than those of land use intensification. The quasi-perched nature of Lake Rerewhakaaitu likely confers some resilience to land use changes in both the topographic and the hydrologically effective catchment, but also results in limited options for catchment management to offset the effects of a warming climate, which will increase the frequency of duration of stratification events. Additional countermeasures such as destratification or oxygenation may be required in the future to present climate-related deterioration of lake water quality but not until options are exhausted to reduce yields of nutrients from riparian areas and the hydrologically effective catchment.

References

Armiento, G., Baiocchi, A., Cremisini, C., Crovato, C., Lotti, F., Lucentini, L., Mazzuoli, M., Nardi, E., Piscopo, V., Proposito, M. and Veschetti, E. (2015). An integrated approach to identify water resources for human consumption in an area affected by high natural arsenic content. Water. 7(9), 5091-5114.

Ascough Ii, J.C., Maier, H.R., Ravalico, J.K. and Strudley, M.W. (2008). Future research challenges for incorporation of uncertainty in environmental and ecological decision-making. Ecological Modelling. 219(3–4), 383-399.

Ayenew, T. and Tilahun, N. (2008). Assessment of lake–groundwater interactions and anthropogenic stresses, using numerical groundwater flow model, for a Rift lake catchment in central Ethiopia. Lakes & Reservoirs: Research & Management. 13(4), 325-343.

Baiocchi, A., Dragoni, W., Lotti, F., Luzzi, G. and Piscopo, V. (2006). Outline of the hydrogeology of the Cimino and Vico volcanic area and of the interaction between ground water and Lake Vico (Lazio region, central Italy). Bollettino della Societa Geologica Italiana. 125(2), 187-202.

Bruce, L.C., Hamilton, D., Imberger, J., Gal, G., Gophen, M., Zohary, T. and Hambright, K.D. (2006). A numerical simulation of the role of zooplankton in C, N and P cycling in Lake Kinneret, Israel. Ecological Modelling. 193(3), 412-436.

Burger, D.F., Hamilton, D.P. and Pilditch, C.A. (2008). Modelling the relative importance of internal and external nutrient loads on water column nutrient concentrations and phytoplankton biomass in a shallow polymictic lake. Ecological Modelling. 211(3–4), 411-423.

Burns, N., McIntosh, J. and Scholes, P. (2009). Managing the lakes of the Rotorua District, New Zealand. Lake and Reservoir Management. 25(3), 284-296.

Chapman, M.A., Jolly, V.H. and Flint, E.A. (1981). Limnology of Lake Rerewhakaaitu. New Zealand Journal of Marine and Freshwater Research. 15(2), 207-224.

Chikita, K.A., Nishi, M., Fukuyama, R. and Hamahara, K. (2004). Hydrological and chemical budgets in a volcanic caldera lake: Lake Kussharo, Hokkaido, Japan. Journal of Hydrology. 291(1–2), 91-114.

Cho, E., Arhonditsis, G.B., Khim, J., Chung, S. and Heo, T.-Y. (2016). Modeling metal-sediment interaction processes. Environmental Modelling & Software. 80(C), 159-174.

Collins, A.L. and McGonigle, D.F. (2008). Monitoring and modelling diffuse pollution from agriculture for policy support: UK and European experience. Environmental Science & Policy. 11(2), 97-101.

D'Arcy, B. and Frost, A. (2001). The role of best management practices in alleviating water quality problems associated with diffuse pollution. Science of The Total Environment. 265(1–3), 359-367.

Dada, A.C. and Hamilton, D.P. (2016). Predictive models for determination of *E. coli* Concentrations at inland recreational beaches. Water, Air, & Soil Pollution. 227(9), 347.

Davies-Colley, R.J. (2013). River Water Quality in New Zealand: An Introduction and Overview, Manaaki Whenua Press, Lincoln, New Zealand.

Fish, G.R. (1978). Lake Rerewhakaaitu -an apparently phosphate-free lake. New Zealand Journal of Marine and Freshwater Research. 12(3), 257-263.

Gömann, H., Kreins, P., Kunkel, R. and Wendland, F. (2005). Model based impact analysis of policy options aiming at reducing diffuse pollution by agriculture—a case study for the river Ems and a sub-catchment of the Rhine. Environmental Modelling & Software. 20(2), 261-271.

Hamilton, D.P. (2014). Memo: Nutrient Budget for Lake Tarawera. http://www.rotorualakes.co.nz/vdb/document/831 (accessed Dec 4, 2017)

Hamilton, D.P., Collier, K.J. and Howard-Williams, C. (2016a). Lake restoration in New Zealand. Ecological Management & Restoration. 17(3), 191-199.

Hamilton, D.P., Salmaso, N. and Paerl, H.W. (2016b). Mitigating harmful cyanobacterial blooms: strategies for control of nitrogen and phosphorus loads. Aquatic Ecology. 50(3), 351-366.

Hamilton, D.P. and Schladow, S.G. (1997). Prediction of water quality in lakes and reservoirs. Part I — Model description. Ecological Modelling. 96(1), 91-110.

Heathwaite, A.L., Quinn, P.F. and Hewett, C.J.M. (2005). Modelling and managing critical source areas of diffuse pollution from agricultural land using flow connectivity simulation. Journal of Hydrology. 304(1–4), 446-461.

Hipel, K.W. and McLeod, A.I. (1994). Time Series Modelling of Water Resources and Environmental Systems. Developments in Water Science, Volume 45, Elsevier.

Howard-Williams, C., Davies-Colley, R.J., Rutherford, K. and Wilcock, R. (2010). Diffuse pollution and freshwater degradation: New Zealand approaches to solutions. 14th International Conference of the Inernational Water Assoication Diffuse Pollution Specialist Group, DIPCON 2010.

Imberger, J. and Patterson, J.C. (1981). A dynamic reservoir simulation model: DYRESM5, Academic press.

Irwin, J. (1970). Lake Rerewhakaaitu, Provisional Bathymetry, 1:7,920. N.Z. Oceangr. Inst. Chart Lake Series.

Jensen, H.S. and Andersen, F.O. (1992). Importance of temperature, nitrate and pH for phosphate release from aerobic sediments of four shallow, eutrophic lakes. Limnology and Oceanography. 37(3), 577–589.

Jaworska-Szulc, B. (2016). Role of the Lakes in groundwater recharge and discharge in the Young Glacial Area, Northern Poland. Groundwater. 54(4), 603-611.

Jeppesen, E., Kronvang, B., Meerhoff, M., Søndergaard, M., Hansen, K.M., Andersen, H.E., Lauridsen, T.L., Liboriussen, L., Beklioglu, M., Özen, A. and Olesen, J.E. (2009). Climate change effects on runoff, catchment phosphorus loading and lake ecological state, and potential adaptations. Journal of Environmental Quality. 38(5), 1930-1941.

Jones, H.F.E., Özkundacki, D., McBride, C., Allan, M.G., Faber, J., Pilditch, C.A. and Hamilton, D.P. (2012). Waituna Lagoon modelling: Developing quantitative assessments to assist with lagoon management. Environmental Research Institute Report 004, University of Waikato, Hamilton.

Kendall, M.G. (1975). Rank Correlation Methods (4th ed.), Charles Griffin, London.

Kim, G., Yur, J. and Kim, J. (2007). Diffuse pollution loading from urban stormwater runoff in Daejeon City, Korea. Journal of Environmental Management. 85(1), 9-16.

LINZ (2012a). NZ 8m Digital Elevation Model. Land Information New Zealand. https://data.linz.govt.nz/layer/51768-nz-8m-digital-elevation-model-2012/ (accessed Dec. 4, 2017)

LINZ (2012b). NZ Topo50 Maps: 1:50,000: BF38. Land Information New Zealand. https://www.linz.govt.nz/land/maps/topographic-maps/topo50-maps (accessed Dec. 4, 2017)

Liu, G.D., Wu, W.L. and Zhang, J. (2005). Regional differentiation of non-point source pollution of agriculture-derived nitrate nitrogen in groundwater in northern China. Agriculture, Ecosystems & Environment. 107(2–3), 211-220.

LUCAS (2016). LUCAS New Zealand Land Use Map. Ministry for the Environment. https://data.mfe.govt.nz/layer/52375-lucas-nz-land-use-map-1990-2008-2012-v016/ (accessed Dec. 4, 2017)

MacKay, M.D., Neale, P.J., Arp, C.D., De Senerpont Domis, L.N., Fang, X., Gal, G., Jöhnk, K.D., Kirillin, G., Lenters, J.D., Litchman, E., MacIntyre, S., Marsh, P., Melack, J., Mooij, W.M., Peeters, F., Quesada, A., Schladow, S.G., Schmid, M., Spence, C. and Stokesr, S.L. (2009). Modeling lakes and reservoirs in the climate system. Limnology and Oceanography. 54, 2315-2329.

Mann, H.B. (1945). Nonparametric tests against trend. Econometrica. 13(3), 245-259.

McColl, R.H.S. (1972). Chemistry and trophic status of seven New Zealand lakes. New Zealand Journal of Marine and Freshwater Research. 6(4), 399-447.

McDowell, R.W. and Hawke, M.F. (2006). Assessment of a novel technique to remove phosphorus from streamflow. Environment Bay of Plenty.

McIntosh, J. (2012). Lake Rerewhakaaitu nutrient budget. Bay of Plenty Regional Council.

McIntosh, J.J., Ngapo, N., Stace, C.E., Ellery, G.R. and Gibbons-Davies, J. (2001). Lake Rerewhakaaitu Project. Environment Bay of Plenty Report 2001/15.

Me, W., Abell, J.M. and Hamilton, D.P. (2015). Effects of hydrologic conditions on SWAT model performance and parameter sensitivity for a small, mixed land use catchment in New Zealand. Hydrology and Earth System Sciences. 19(10), 4127-4147.

Mohseni, O., Stefan, H.G. and Erickson, T.R. (1998). A nonlinear regression model for weekly stream temperatures. Water Resources Research. 34(10), 2685-2692.

Özkundakci, D., Hamilton, D.P., McDowell, R. and Hill, S. (2013). Phosphorus dynamics in sediments of a eutrophic lake derived from 31P nuclear magnetic resonance spectroscopy. Marine and Freshwater Research. 65(1), 70-80.

Paerl, H.W. and Huisman, J. (2009). Climate change: a catalyst for global expansion of harmful cyanobacterial blooms. Environmental Microbiology Reports. 1(1), 27-37.

Parfitt, R.L., Baisden, W.T., Schipper, L.A. and Mackay, A.D. (2008a). Nitrogen inputs and outputs for New Zealand at national and regional scales: Past, present and future scenarios. Journal of the Royal Society of New Zealand. 38(2), 71-87.

Parfitt, R.L., Baisden, W.T. and Elliott, A.H. (2008b). Phosphorus inputs and outputs for New Zealand in 2001 at national and regional scales. Journal of the Royal Society of New Zealand. 38(1), 37-50.

Park, S.S. and Lee, Y.S. (2002). A water quality modeling study of the Nakdong River, Korea. Ecological Modelling. 152(1), 65-75.

Patten, B.C., Egloff, D.A. and Richardson, T.H. (1975) Total Ecosystem Model for a Cove in Lake Texoma, Academic Press.

PCE (2004). Growing for good: Intensive farming, sustainability and New Zealand's environment, Parliamentary Commissioner for the Environment, Wellington.

Pereira, S.A., Trindade, C.R.T., Albertoni, E.F. and Palma-Silva, C. (2012). Aquatic macrophytes as indicators of water quality in subtropical shallow lakes, Southern Brazil. Acta Limnologica Brasiliensia. 24(1), 52-63.

PMCSA (2017). New Zealand's fresh waters: Values, state, trends and human impacts, Office of the Prime Minister's Chief Science Advisor, Wellington.

Reeves, R.R., Morgenstern, U., Daughney, C.J., Stewart, M.K. and Gordon, D. (2008). Identifying leakage to groundwater from Lake Rerewhakaaitu using isotopic and water quality data. Journal of Hydrology (New Zealand). 47(2), 85-106.

Rose, J.L., Moreau-Fournier, M., van der Raaij, R., Tschritter, C., Rosenberg, M. and Zemansky, G. (2012). Lake Tarawera groundwater investigation phase 2. GNS Science Consultancy Report 2011/326, 251p.

Schladow, S.G. and Hamilton, D.P. (1997). Prediction of water quality in lakes and reservoirs: Part II - Model calibration, sensitivity analysis and application. Ecological Modelling. 96(1), 111-123.

Scholes, P. and Hamill, K. (2016). Rotorua Lakes Water Quality Report 2014/2015. Bay of Plenty Regional Council.

Shoemaker, L., Dai, T. and Koenig, J. (2005). TMDL Model Evaluation and Research Needs, U.S. Environmental Protection Agency, Washington DC.

Spigel, R.H., Imberger, J. and Rayner, K.N. (1986) Modeling the diurnal mixed layer. Limnology and Oceanography 31(3), 533-556.

Smith, V.H., Wood, S.A., McBride, C.G., Atalah, J., Hamilton, D.P. and Abell, J. (2016). Phosphorus and nitrogen loading restraints are essential for successful eutrophication control of Lake Rotorua, New Zealand. Inland Waters. 6(2), 273-283.

Tait, A., Henderson, R., Turner, R. and Zheng, X. (2006). Thin plate smoothing spline interpolation of daily rainfall for New Zealand using a climatological rainfall surface. International Journal of Climatology. 26(14), 2097-2115.

Vant, W.N. (1987). Lake Managers Handbook. Published for the National Water and Soil Conservation Authority by the Water and Soil Directorate, Ministry of Works and Development, Wellington, N.Z.

Viner, A. B. (Ed.). (1987). Inland waters of New Zealand (Vol. 241). Science Information Pub. Centre, Department of Scientific and Industrial Research.

Wang, J.L. and Yang, Y.S. (2008). An approach to catchment-scale groundwater nitrate risk assessment from diffuse agricultural sources: a case study in the Upper Bann, Northern Ireland. Hydrological Processes. 22(21), 4274-4286.

White, P., Toews, M., Tschritter, C. and Lovett, A. (2015). Nitrogen discharge from the groundwater system to lakes and streams in the greater Lake Tarawera catchment. GNS Science Consultancy Report 2015/108.

White, P.A., Nairn, I.A., Tait, T. and Reeves, R.R. (2003). Groundwater in the Lake Rerewhakaaitu catchment. Environment Bay of Plenty.

Woods, R., Hendrikx, J., Henderson, R. and Tait, A. (2006). Estimating mean flow of New Zealand rivers. Journal of Hydrology (New Zealand). 45(2), 95-109.

Wunderlich, W.O. (1972). Heat and mass transfer between a water surface and the atmosphere, Tennessee Valley Authority, Office of Natural Resources and Economic Development, Division of Air and Water Resources, Water Systems Development Branch.

Yang, J., McMillan, H. and Zammit, C. (2017a). Modeling surface water–groundwater interaction in New Zealand: Model development and application. Hydrological Processes. 31(4), 925-934.

Yang, Z., Zhou, Y., Wenninger, J., Uhlenbrook, S., Wang, X. and Wan, L. (2017b). Groundwater and surface-water interactions and impacts of human activities in the Hailiutu catchment, northwest China. Hydrogeology Journal. 25(5), 1341-1355.

Yeates, P.S. and Imberger, J. (2003) Pseudo two-dimensional simulations of internal and boundary fluxes in stratified lakes and reservoirs. International Journal of River Basin Management. 1(4), 297-319.

Yin, C., Li, Y. and Urich, P. (2013). SimCLIM 2013 Data Manual. CLIMsystems.

Ziemińska-Stolarska, A. and Skrzypski, J. (2012). Review of mathematical models of water quality. Ecological Chemistry and Engineering S. 19(2), 197-211.